

A Phase Model with Large Time Delayed Coupling^{*}

Isam Al-Darabsah^{*,†}

Sue Ann Campbell^{*,‡}

Abstract

We consider two identical oscillators with weak, time delayed coupling. We start with a general system of delay differential equations then reduce it to a phase model. With the assumption of large time delay, the resulting phase model has an explicit delay and phase shift in the argument of the phases and connection function, respectively. Using the phase model, we prove that for any type of oscillators and any coupling, the in-phase and anti-phase phase-locked solutions always exist and give conditions for their stability. We show that for small delay these solutions are unique, but with large enough delay multiple solutions of each type with different frequencies may occur. We give conditions for the existence and stability of other types of phase-locked solutions. We discuss the various bifurcations that can occur in the phase model as the time delay is varied. The results of the phase model analysis are applied to Morris-Lecar oscillators with diffusive coupling and compared with numerical studies of the full system of delay differential equations. We also consider the case of small time delay and compare the results with the existing ones in the literature.

Keywords: Coupled oscillators · Large time delay · Synchronization · Phase-locking

1 Introduction

Coupled oscillator models have been used to study different aspects of biology, chemistry and engineering, for example chemical waves [1], flashing of fireflies [2], laser arrays [3, 4], power system networks [5], neural networks [6–9], movement of a slime mold [10], and coupled predator-prey systems [11, 12]. Time delays in the connections between the oscillators are inescapable due to the time for a signal to propagate from one element to the other. Many of these systems exhibit phase-locking behaviour, i.e., all the oscillators have similar waveforms and frequencies, but with some fixed phase difference between different oscillators. To study the existence and stability of such phase-locked solutions and how they are related to the time delay and other parameters, one must formulate a model for the system. We discuss two approaches below.

One approach to study connected networks of oscillators is through phase models [13]. In these models, each oscillator is represented only by its phase along its limit cycle, with amplitude variation neglected [14–16]. Phase models take the general form [14, 17]:

$$\frac{d\theta_i}{d\xi} = \Omega_i + H_i(\theta_1(\xi), \dots, \theta_n(\xi)), \quad i = 1, \dots, n, \quad (1)$$

^{*}This research is supported in part by the Natural Sciences and Engineering Research Council of Canada.

^{*}Department of Applied Mathematics, University of Waterloo, Waterloo, ON, N2L 3G1, Canada.

[†]Email: ialdarabsah@uwaterloo.ca

[‡]Email: sacampbell@uwaterloo.ca

where $\theta_i \in [0, 2\pi)$ is the phase of the i^{th} oscillator, $\Omega_i > 0$ the natural frequency and H_i are the connection functions. Motivated by the famous *Kuramoto model* [1], in the literature the functions H_i often take the form:

$$H_i(\theta_1(\xi), \dots, \theta_n(\xi)) = \sum_{j=1}^n K_{ij} H(\theta_j(\xi) - \theta_i(\xi)), \quad i = 1, \dots, n, \quad (2)$$

where K_{ij} is the adjacency matrix of an unweighted network [15, 18]. In the original Kuramoto model [1] the function H in (2) is the sine function. Usually, transmission time delay is introduced as an explicit delay in the argument of the phases [18–23]:

$$\frac{d\theta_i}{d\xi} = \Omega_i + \sum_{j=1}^n K_{ij} H(\theta_j(\xi - \tau) - \theta_i(\xi)), \quad i = 1, \dots, n. \quad (3)$$

Most studies of this model focus only on synchronization [18] or use simplifications such as $H(\cdot) = \sin(\cdot)$ [19–24] or $n = 2$ [19, 22, 23].

Other authors introduce additional processes into system (3). For instance, in [19], the dynamic behavior of coupled oscillators with time delayed interaction under a pinning force is studied. In [21, 22], the authors study time delayed phase models with $H = \sin(\cdot)$ and random noise forcing. Finally, a *phase shift* is sometimes included in the model of a network of connected oscillators to represent the temporal distance between the oscillators. In general, the phase shift between two oscillators α_{ij} is incorporated in the phase model as, see e.g., [24–26],

$$\frac{d\theta_i}{d\xi} = \Omega_i + \sum_{j=1}^n K_{ij} H(\theta_j(\xi) - \theta_i(\xi) - \alpha_{ij}), \quad i = 1, \dots, n. \quad (4)$$

In the case where $H(\cdot) = \sin(\cdot)$ this model is called the Kuramoto-Sakaguchi model [26]. In fact, there is a relation between such phase shifts and the transmission time delay. In [27, 28], the authors have shown how the model with delay and the model with the phase shift are linked. We will review the details of this link later in this section.

Models of coupled oscillators are also formulated as physically or biological derived differential equations [11, 12, 17]. These models are of the form

$$\frac{d\mathbf{X}_i}{d\rho} = \mathbf{F}_i(\mathbf{X}_i(\rho)) + \epsilon \mathbf{G}_i(\mathbf{X}_1(\rho), \dots, \mathbf{X}_i(\rho), \dots, \mathbf{X}_n(\rho)), \quad i = 1, \dots, n, \quad \mathbf{X}_i \in \mathbb{R}^m, \quad (5)$$

and are such that when $\epsilon = 0$ the dynamical system of each uncoupled oscillator has an exponentially asymptotically stable T_i -periodic limit cycle with corresponding (natural) frequency Ω_i . In these models, \mathbf{X}_i represents the state of the i^{th} oscillator of the system, \mathbf{G}_i are the coupling functions and $\epsilon > 0$ is the coupling strength [14, 27, 29, 30]. Note that \mathbf{X}_i is a vector of dimension at least 2, but can be high dimensional. For example, in a pendulum model \mathbf{X}_i represents the position and velocity of the i^{th} pendulum, while in a neural model \mathbf{X}_i represents the voltage and gating variables of the i^{th} neuron.

If the coupling is weak, $0 < \epsilon \ll 1$, then the theory of weakly coupled oscillators can be used to connect the physical model (5) to a phase model [8, 29–32]. More precisely, the dynamics of each oscillator in the network can be rigorously reduced to a single equation that indicates how the phase of the oscillator changes in time [14, 16, 27]. One form of weakly coupled oscillator theory is *Malkin's Theorem* where the connection functions in the phase model are determined explicitly in terms of \mathbf{G}_i and the limit cycles of the uncoupled system, (5) with $\epsilon = 0$. Let $\varphi_i(t) \in \mathbb{S}^1$ be the

phase deviation of the i^{th} oscillator of (5), i.e., the change in the phase due to the coupling. It then follows from Malkin's Theorem (see e.g., [14, Theorem 9.2]) that the dynamics of (5) can be described by the phase deviation model:

$$\frac{d\varphi_i}{dt} = H_i(\varphi_1(t) - \varphi_i(t), \dots, \varphi_n(t) - \varphi_i(t)) + \mathcal{O}(\epsilon), \quad i = 1, \dots, n, \quad (6)$$

where H_i are the phase interaction functions and the variable $t := \epsilon\rho$ represents slow time because the phase deviations φ_i are slow variables. The references [14, 16, 30] provide other forms of the theory and give further references. We also refer the reader to the recent articles [33–35] for an overview of various numerical and analytical techniques for phase reduction. In [27], Izhikevich generalizes Malkin's theorem to weakly connected oscillators with fixed delay, τ , in their interaction:

$$\frac{d\mathbf{X}_i}{d\rho} = \mathbf{F}_i(\mathbf{X}_i(\rho)) + \epsilon\mathbf{G}_i(\mathbf{X}_1(\rho - \tau), \dots, \mathbf{X}_i(\rho - \tau), \dots, \mathbf{X}_n(\rho - \tau)), \quad i = 1, \dots, n, \quad \mathbf{X}_i \in \mathbb{R}^m \quad (7)$$

where all uncoupled oscillators have nearly identical natural frequencies. Assuming the natural frequency is 1, Izhikevich shows that the phase deviation model corresponding to (7) is

$$\frac{d\varphi_i}{dt} = H_i(\varphi_1(t - \eta) - \varphi_i(t) - \zeta, \dots, \varphi_n(t - \eta) - \varphi_i(t) - \zeta) + \mathcal{O}(\epsilon), \quad i = 1, \dots, n, \quad (8)$$

where $\eta := \epsilon\tau$ and $\zeta := \tau \bmod 2\pi$. The functions H_i are still defined explicitly in terms of \mathbf{G}_i and the uncoupled limit cycle in (7). It is clear that the time delay τ enters the phase model (8) as both an explicit delay, η , and a phase shift, ζ . The major result that Izhikevich proved in [27] is that if the delay τ in (7) satisfies $\epsilon\tau = \mathcal{O}(1)$ (large delay), then the explicit delay occurs in the phase model (8). However, when the delay satisfies $\tau = \mathcal{O}(1)$ with respect to ϵ (small delay), no delay appears in the argument of the phases. Hence, (8) becomes:

$$\frac{d\varphi_i}{dt} = H_i(\varphi_1(t) - \varphi_i(t) - \zeta, \dots, \varphi_n(t) - \varphi_i(t) - \zeta) + \mathcal{O}(\epsilon), \quad i = 1, \dots, n. \quad (9)$$

We refer the reader to the review article [24] and the references therein for different scenarios where large or small delay appears in-phase models.

In this article we focus on physical models with the following particular form

$$\frac{d\mathbf{X}_i}{d\rho} = \mathbf{F}(\mathbf{X}_i(\rho)) + \epsilon \sum_{j=1}^n K_{ij} \mathbf{G}(\mathbf{X}_i(\rho), \mathbf{X}_j(\rho - \tau)), \quad i = 1, \dots, n, \quad \mathbf{X}_i \in \mathbb{R}^m \quad (10)$$

where $K_{ii} = 0$. This represent the following modelling assumptions. The oscillators are identical. The coupling occurs pairwise between the oscillators and there is no coupling from an oscillator to itself. The coupling to the i^{th} oscillator occurs close to that oscillator, so the time delay represents the time it takes for information to travel from the j^{th} oscillator to the i^{th} oscillator. Models with such structure occur in models of biological systems [8, 11].

Assuming the uncoupled oscillators in (10) have a natural frequency Ω and the $K_{ij} = \mathcal{O}(1)$ with respect to ϵ , we show in the appendix that the approach of [27] can be applied to yield

$$\frac{d\varphi_i}{dt} = \frac{1}{\Omega} \sum_{j=1}^n K_{ij} H(\varphi_j(t - \eta) - \varphi_i(t) - \zeta) + \mathcal{O}(\epsilon) \quad (11)$$

where $\eta := \epsilon\Omega\tau$ and $\zeta := \Omega\tau \bmod 2\pi$, in the case of large delay, i.e., when $\epsilon\Omega\tau = \mathcal{O}(1)$. In the case of small delay (11) becomes

$$\frac{d\varphi_i(t)}{dt} = \frac{1}{\Omega} \sum_{j=1}^n K_{ij} H(\varphi_j(t) - \varphi_i(t) - \Omega\tau) + \mathcal{O}(\epsilon). \quad (12)$$

To see how the phase deviation model relates to the standard phase model, note that the phase of oscillations θ_i in (10) have the form:

$$\theta_i(\xi) = \Omega\xi + \varphi_i(t), \quad i = 1, \dots, n, \quad (13)$$

where $t = \epsilon\Omega\xi$, see [14, 27]. Notice that the natural frequency of each uncoupled oscillator in (13) is Ω . Then,

$$\frac{d\theta_i}{d\xi} = \Omega + \epsilon\Omega \frac{d\varphi_i}{dt} = \Omega + \epsilon \sum_{j=1}^n K_{ij} H(\theta_j(\xi - \tau) - \theta_i(\xi)) + \mathcal{O}(\epsilon^2). \quad (14)$$

Similarly, when the time delay is small, we have

$$\frac{d\theta_i}{d\xi} = \Omega + \epsilon \sum_{j=1}^n K_{ij} H(\theta_j(\xi) - \theta_i(\xi) - \zeta) + \mathcal{O}(\epsilon^2). \quad (15)$$

Thus in the phase model formulation, the coupling strength parameter ϵ explicitly appears in front of the connection function h . Regarding the dynamics, it follows from (13) that

$$\theta_{i+1} - \theta_i = \varphi_{i+1} - \varphi_i, \quad i = 1, \dots, n-1$$

i.e., phase-locked solutions are the same as phase deviation locked solutions [14]. The existence and stability of phase-locked solutions of system (15) has been studied in the case of two oscillators [24, 36] and many oscillators with structured coupling [17, 24, 37].

The goals in this paper are twofold. First, the majority of studies of coupled oscillators with large delays have been done in the context of isolated phase models, often with just sine function coupling. Thus we will revisit and extend this analysis in the case where the phase model is explicitly connected to a physical differential equation model and the function H is general. In particular, we will show that the multiple stable phase-locked solutions of the same type may occur even when the coupling is weak. Second, note that the small delay phase deviation model (12) is a system of ordinary differential equations, while the large delay model (10) is a delay differential equation model. Thus the spectrum of Floquet multipliers of a periodic solution is finite for the former and countably infinite for the latter. Nevertheless, several studies have verified numerically that the model (12) gives an accurate description of existence and stability of phase-locked periodic solutions of (5) in the case of weak coupling and small delay [17, 36]. Here we will show why this is the case. In particular we will show how the solutions of system (10) reduce to those of system (12) if the delay is small. In this article, we will focus on (10) when $n = 2$ as this is enough to illustrate our main points.

The paper is organized as follows. In the next section, we reduce the model of two weakly connected oscillators with large time delay to a phase model, and study the existence of phase-locked solutions. In Section 3, we give a complete description of the stability criteria for all phase-locked solutions and describe the potential bifurcations that can occur in the system. Then we compare our results with the stability criteria in [36] when the time delay is small. In Section 4, we consider a particular application to Morris-Lecar oscillators with diffusive coupling. Numerically,

we derive the corresponding phase model, calculate the phase-locked solutions, determine their stability and explore the existence of bifurcations. We also compare prediction of the phase model and solutions of the full model. Finally, we examine the behaviour when the time delay is small. In Section 5, we discuss our results.

2 Phase Model

Consider the system of ODEs

$$\frac{d\mathbf{X}_i}{d\rho} = \mathbf{F}(\mathbf{X}_i(\rho)) \quad i = 1, 2, \quad \mathbf{X}_i \in \mathbb{R}^n. \quad (16)$$

Assume that the system (16) admits an exponentially asymptotically stable periodic orbit given by $\mathbf{X} = \hat{\mathbf{X}}(\rho)$ with natural frequency Ω , $0 \leq \rho \leq T = 2\pi/\Omega$.

Next, consider a weakly connected system of two identical coupled oscillators of the form (16) with time delayed coupling:

$$\begin{aligned} \frac{d\mathbf{X}_1}{d\rho} &= \mathbf{F}(\mathbf{X}_1(\rho)) + \epsilon \mathbf{G}(\mathbf{X}_1(\rho), \mathbf{X}_2(\rho - \tau); \epsilon), \\ \frac{d\mathbf{X}_2}{d\rho} &= \mathbf{F}(\mathbf{X}_2(\rho)) + \epsilon \mathbf{G}(\mathbf{X}_2(\rho), \mathbf{X}_1(\rho - \tau); \epsilon), \end{aligned} \quad (17)$$

where $\mathbf{G} : \mathbb{R}^n \times \mathbb{R}^n \rightarrow \mathbb{R}^n$ describes the coupling between the two oscillators and ϵ is the coupling strength. Assume that ϵ is sufficiently small and $\eta := \epsilon\Omega\tau = \mathcal{O}(1)$. Let $t = \epsilon\rho$ be slow time and $\varphi_i(t) \in \mathbb{S}^1$ be the phase deviation from the natural oscillation $\hat{X}(\rho)$, $\rho \geq 0$. Then, by applying weakly coupled oscillator theory with delayed interactions in [27], $(\varphi_1, \varphi_2)^T \in \mathbb{T}^2$ is a solution to

$$\begin{aligned} \frac{d\varphi_1}{dt} &= \frac{1}{\Omega} H(\varphi_2(t - \eta) - \varphi_1(t) - \Omega\tau) + \mathcal{O}(\epsilon), \\ \frac{d\varphi_2}{dt} &= \frac{1}{\Omega} H(\varphi_1(t - \eta) - \varphi_2(t) - \Omega\tau) + \mathcal{O}(\epsilon), \end{aligned} \quad (18)$$

where H is a 2π -periodic function defined by

$$H(\phi) = \frac{1}{2\pi} \int_0^{2\pi} \hat{\mathbf{Z}}(\rho)^T \mathbf{G}(\hat{\mathbf{X}}(\rho), \hat{\mathbf{X}}(\rho + \phi)) d\rho. \quad (19)$$

Here $\hat{\mathbf{Z}}(\rho)$ is the unique nontrivial 2π -periodic solution to the adjoint linear system

$$\frac{d\hat{\mathbf{Z}}}{d\rho} = -[D\mathbf{F}(\hat{\mathbf{X}}(\rho))]^T \hat{\mathbf{Z}}$$

satisfying the normalization condition

$$\frac{1}{2\pi} \int_0^{2\pi} \hat{\mathbf{Z}}(\rho) \cdot \mathbf{F}(\hat{\mathbf{X}}(\rho)) d\rho = 1.$$

The derivation of system (18) from (17) follows from the Appendix with $n = 2$ and $K_{12} = K_{21} = 1$.

Dropping the terms $\mathcal{O}(\epsilon)$ in (18), we obtain the phase deviation model:

$$\begin{aligned}\frac{d\varphi_1}{dt} &= \frac{1}{\Omega} H(\varphi_2(t - \eta) - \varphi_1(t) - \Omega\tau), \\ \frac{d\varphi_2}{dt} &= \frac{1}{\Omega} H(\varphi_1(t - \eta) - \varphi_2(t) - \Omega\tau).\end{aligned}\tag{20}$$

For simplicity, in the rest of the paper we will refer to (20) as the *phase model* instead of the phase deviation model.

We study the dynamics of the model (20) by exploring *phase locking* in (20), that is, solutions of (20) such that $\varphi_2 - \varphi_1 = \text{constant}$ [14]. We suppose that

$$\varphi_1(t) = \omega t \quad \text{and} \quad \varphi_2(t) = \omega t + \psi\tag{21}$$

where ω is the frequency deviation of the oscillator and ψ is the natural phase difference [14]. Substituting (21) into (20) leads to

$$\begin{aligned}\omega - \frac{1}{\Omega} H(\psi - \omega\eta - \Omega\tau) &= 0, \\ \omega - \frac{1}{\Omega} H(-\psi - \omega\eta - \Omega\tau) &= 0.\end{aligned}\tag{22}$$

We rewrite this as

$$F(\omega, \psi) = 0 = F(\omega, -\psi)\tag{23}$$

where

$$F(\omega, \cdot) := \omega - \frac{1}{\Omega} H(\cdot - \omega\eta - \Omega\tau).\tag{24}$$

In this article, we are interested in exploring how the solutions (ψ and ω) of (22) vary with τ when the coupling strength (ϵ) and frequency (Ω) are fixed. Note that, we need only to investigate ψ in $[0, 2\pi)$, due to the 2π periodicity of H , and $\omega \in \mathbb{R}$.

First, by subtracting the equations of (22), we obtain

$$H(\psi - \omega\eta - \Omega\tau) - H(-\psi - \omega\eta - \Omega\tau) = 0.\tag{25}$$

Since H is 2π -periodic function, equation (25) always has the solutions $\psi = 0, \pi$. The corresponding frequency deviation is determined from the equation

$$F(\omega, 0) = \omega - \frac{1}{\Omega} H(-\omega\eta - \Omega\tau) = 0\tag{26}$$

when $\psi = 0$ and

$$F(\omega, \pi) = \omega - \frac{1}{\Omega} H(\pi - \omega\eta - \Omega\tau) = 0\tag{27}$$

when $\psi = \pi$.

Equations (26) and (27) are guaranteed to have a least one solution due to the continuity and 2π periodicity of H . In fact, if τ is sufficiently large, they may have multiple solutions. To see this, recall that $\eta = \epsilon\omega\tau$ and note that

$$F_\omega(\omega, 0) = 1 + \epsilon\tau H'(-\omega\epsilon\Omega\tau - \Omega\tau),\tag{28}$$

where F_ω is the partial derivative of F with respect to ω . If there exists $\bar{\omega}$ such that $F(\bar{\omega}, 0) = 0$ and $F_\omega(\bar{\omega}, 0) < 0$ then (26) has more than one solution. Similar arguments apply to equation (27). This may be possible if τ is sufficiently large.

Remark 2.1. The solutions $\psi^* = 0$ and $\psi^* = \pi$ of (25) correspond to **in-phase** and **anti-phase** periodic solutions of the original model (17), respectively. By in-phase solution we mean both oscillators reach their highest peak at the same time, whereas an anti-phase solution means one oscillator reaches its highest peak one half-period after the other oscillator. Examples of these solutions are given in Figure 1.

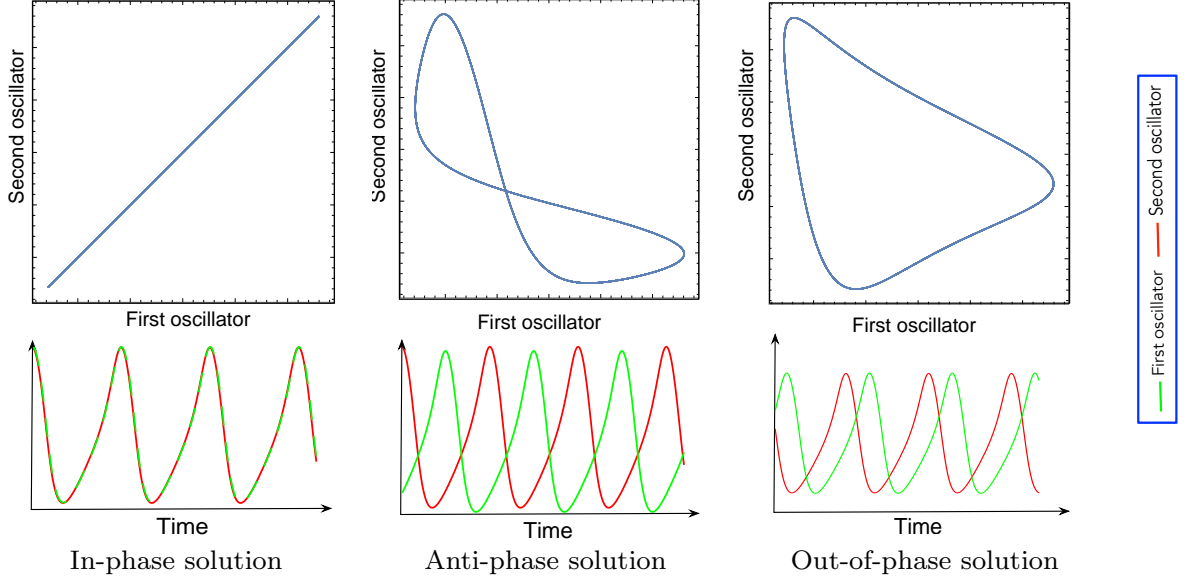


Figure 1: Illustrations of the phase-locked dynamics of model (17).

In fact, system (17) could have other phase-locked solutions (neither in-phase nor anti-phase) corresponding to the solutions ψ of (22) such that $\psi \notin \{0, \pi\}$. As in [38], we will refer to these solutions of (17) as **out-of-phase** solutions. Let (ω^*, ψ^*) be a solution of (22) at $\tau = \tau^*$ such that $\psi^* \notin \{0, \pi\}$. Then ω^* and ψ^* satisfy (23), that is, (ω^*, ψ^*) is an intersection point of the contours $F(\omega, \psi) = 0$ and $F(\omega, -\psi) = 0$ in the $\omega\psi$ -plane. Suppose that $\psi^* \in (0, \pi)$ with a corresponding ω^* are solutions to (22) at $\tau = \tau^*$, then

$$\frac{1}{\Omega} H(\psi^* - 2\pi - \omega^* \eta^* - \Omega \tau^*) = \frac{1}{\Omega} H(\psi^* - \omega^* \eta^* - \Omega \tau^*) = \omega^*$$

and

$$\frac{1}{\Omega} H(2\pi - \psi^* - \omega^* \eta^* - \Omega \tau^*) = \frac{1}{\Omega} H(-\psi^* - \omega^* \eta^* - \Omega \tau^*) = \omega^*$$

due to the periodicity of H . Thus, $2\pi - \psi^*$ is also a solution in (22) with corresponding ω^* .

This leads to the following.

Proposition 2.1 (Existence of phase-locked solutions). *For any interaction function H and any values of Ω , ϵ and τ the phase model (20) has the solutions $\psi^* = 0$ and $\psi^* = \pi$ with corresponding frequency deviations determined by (26) and (27), respectively. If $\psi^* \in (0, \pi)$ with corresponding ω^* are solutions to (22) at $\tau = \tau^*$ then so is $2\pi - \psi^*$ with ω^* , i.e., solutions come in pairs.*

3 Stability

In this section, we discuss the linear stability of the solutions (21) of (20). The linearization of (20) about the solution (21) is

$$\begin{aligned}\frac{du_1}{dt} &= -au_1(t) + au_2(t - \eta), \\ \frac{du_2}{dt} &= -bu_2(t) + bu_1(t - \eta),\end{aligned}\tag{29}$$

where

$$a = \frac{1}{\Omega} H'(\psi - \omega\eta - \Omega\tau) \quad \text{and} \quad b = \frac{1}{\Omega} H'(-\psi - \omega\eta - \Omega\tau).\tag{30}$$

In (30), H' represents the derivative of H with respect to its argument. It is useful for our analysis to scale time so the delay becomes one. Applying the scaling

$$\eta s = t, U_1(s) = u_1(t), U_2(s) = u_2(t),$$

results in

$$\begin{aligned}\frac{dU_1}{ds} &= -\eta a U_1(s) + \eta a U_2(s - 1), \\ \frac{dU_2}{ds} &= -\eta b U_2(s) + \eta b U_1(s - 1).\end{aligned}\tag{31}$$

It follows that the corresponding characteristic equation is

$$\Delta(\lambda; \eta) = \lambda^2 + \eta(a + b)\lambda + \eta^2 ab - \eta^2 ab e^{-2\lambda} = 0.\tag{32}$$

In the following we study the distribution of roots of this equation.

Proposition 3.1. *Assume $ab = 0$. Then $\Delta(\lambda; \eta)$ has:*

- i. One positive root and one zero root when $a + b < 0$;*
- ii. Two zero roots when $a + b = 0$;*
- iii. One negative root and one zero root when $a + b > 0$.*

Proof. The characteristic equation in this case reduces to

$$\lambda^2 + \eta(a + b)\lambda = 0.$$

The result follows. ■

Proposition 3.2. *$\Delta(\lambda; \eta)$ has a positive real root when one of the following holds.*

- i. $ab > 0$ and $a + b < 0$;*
- ii. $ab < 0$ and $a + b \leq 0$;*
- iii. $ab < 0$, $a + b > 0$ and $a + b + 2\eta ab < 0$.*

Proof. Define

$$f(\lambda) = (\lambda + \eta a)(\lambda + \eta b) \quad \text{and} \quad g(\lambda) = \eta^2 ab e^{-2\lambda}. \quad (33)$$

Then $f(0) = g(0) = \eta^2 ab$ and

$$\Delta(\lambda; \eta) = 0 \quad \iff \quad f(\lambda) = g(\lambda). \quad (34)$$

- i. It follows from $ab > 0$ and $a + b < 0$ that $a < 0$ and $b < 0$. Since (32) is symmetric in a and b , without loss of generality, we may assume $b < a < 0$. Note that $f(-\eta b) = 0 < g(-\eta b)$. Since f is positive and increasing for $\lambda > -\eta b > 0$ and g is positive and decreasing for $\lambda > 0$, there exists $\lambda^* > -\eta b$ such that $f(\lambda^*) = g(\lambda^*)$, see Figure 2a.
- ii. Assume $a > 0$ and $b < 0$. When $a + b < 0$, f is decreasing for $\lambda \in (0, -\frac{a+b}{2}\eta)$ and is increasing for $\lambda > -\frac{a+b}{2}\eta$. Further, g increases for $\lambda > 0$ and $\lim_{\lambda \rightarrow \infty} g(\lambda) = 0$, thus there exists $\lambda^* \in (-\frac{a+b}{2}\eta, -\eta b)$ such that $f(\lambda^*) = g(\lambda^*)$, see Figure 2b. When $a + b = 0$, $f(0) = g(0) = \eta^2 ab$, $f'(0) = 0 < g'(0)$ and f is increasing for $\lambda > 0$. Thus, with the same arguments, λ^* lies in $(0, -\eta b)$.
- iii. Assume $a > 0$ and $b < 0$. In this case f and g are increasing for $\lambda > 0$ and $g < 0$ for $\lambda \geq 0$. Since $f'(0) = \eta(a + b) < -2\eta^2 ab = g'(0)$, then there exists $\lambda^* \in (0, -\eta b)$ such that $f(\lambda^*) = g(\lambda^*)$, see Figure 2c.

■

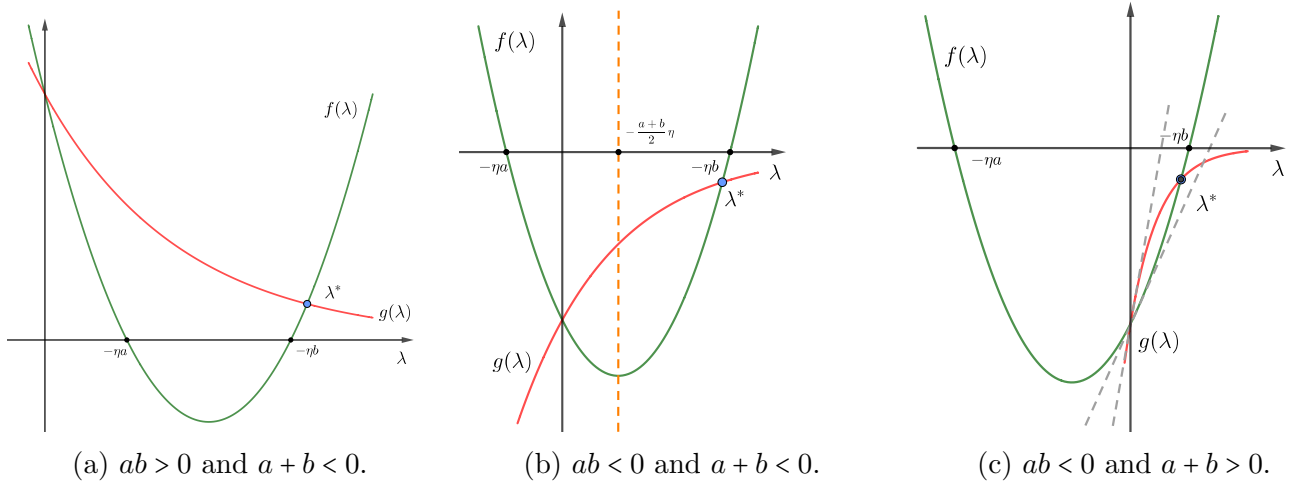


Figure 2: Positive real roots in $\Delta(\lambda; \eta) = 0$.

Proposition 3.3. *When $ab > 0$ and $a + b > 0$, $\Delta(\lambda; \eta)$ has no roots with positive real part.*

Proof. Since $ab > 0$ and $a + b > 0$, we have $a > 0$ and $b > 0$. Assume there is a root $\lambda^* = x + iy$ of $\Delta(\lambda; \eta) = 0$ with $x > 0$. Then, it follows from (33) and (34) that

$$|f(\lambda^*)| = |g(\lambda^*)|. \quad (35)$$

Notice that, due to the positivity of x we get

$$|f(\lambda^*)| = \sqrt{(x + \eta a)^2 + y^2} \sqrt{(x + \eta b)^2 + y^2} > \eta^2 ab$$

and

$$|g(\lambda^*)| = \eta^2 ab e^{-2x} < \eta^2 ab.$$

Hence, $|f(\lambda^*)| > |g(\lambda^*)|$, which contradicts (35). Thus, all roots of $\Delta(\lambda; \eta) = 0$ have nonpositive real parts when $ab > 0$ and $a + b > 0$. ■

Proposition 3.4. $\lambda = 0$ is a root of (32) for any η . If $\eta \neq \eta^* := -\frac{a+b}{2ab}$ then $\lambda = 0$ is a simple root. Otherwise, it is a double root. The double multiplicity of $\lambda = 0$ occurs only in the following cases.

i. $ab > 0$ and $a + b < 0$;

ii. $ab < 0$ and $a + b > 0$.

Proof. It is clear that $\Delta(0; \eta) = 0$ and $\Delta'(0; \eta) = \eta(a + b + 2ab\eta)$ where ' is the derivative with respect to λ . If $\eta \neq \eta^*$ then $\Delta'(0; \eta) \neq 0$, and hence $\lambda = 0$ is a simple root. When $\eta = \eta^*$, we have $\Delta'(0; \eta^*) = 0$ and

$$\Delta''(0; \eta^*) = -\frac{a^2 + b^2}{ab} \neq 0.$$

Thus, $\lambda = 0$ has double multiplicity.

It is clear that η^* exists if and only if

$$-\frac{a+b}{2ab} > 0 \iff \{ab > 0 \text{ and } a + b < 0\} \text{ or } \{ab < 0 \text{ and } a + b > 0\}.$$

■

Proposition 3.5. When $ab < 0$, $a + b > 0$ and $a + b + 2\eta ab \geq 0$, $\Delta(\lambda; \eta)$ has no roots with positive real part.

Proof. Note that the characteristic equation (32) can be written as

$$\Delta(\lambda; \eta) = \lambda^2 + \eta(a + b)\lambda + \eta^2 ab \int_0^2 \lambda e^{-u\lambda} du = 0.$$

Suppose that $\Delta(\lambda; \eta) = 0$ has root $\bar{\lambda}$ with $\text{Re}(\bar{\lambda}) > 0$. Then

$$|\bar{\lambda}(\bar{\lambda} + \eta(a + b))| = \left| \eta^2 ab \bar{\lambda} \int_0^2 e^{-u\bar{\lambda}} du \right| \leq \eta^2 |ab| |\bar{\lambda}| \left| \int_0^2 e^{-u(\text{Re}(\bar{\lambda}))} du \right| \leq 2\eta^2 |ab| |\bar{\lambda}|.$$

Since $ab < 0$ and $a + b + 2\eta ab \geq 0$, we have

$$|\bar{\lambda}(\bar{\lambda} + \eta(a + b))| \leq -2\eta^2 ab |\bar{\lambda}| \leq \eta(a + b) |\bar{\lambda}|$$

which is satisfied if $\bar{\lambda} = 0$ (a contradiction) or

$$|\bar{\lambda} + \eta(a + b)| \leq \eta(a + b).$$

This implies that $\bar{\lambda}$ is in the disk of radius $\eta(a + b)$ centred at the point $-\eta(a + b)$ in the complex plane. Thus, $\text{Re}(\bar{\lambda}) < 0$ or $\bar{\lambda} = 0$. In both cases we arrive at a contradiction. ■

Finally, we show that (32) does not have pure imaginary roots for any value of the parameters.

Proposition 3.6. The characteristic equation (32) has no pure imaginary roots.

Proof. Assume $\lambda = iy$ ($y > 0$) is a root of (32). Separating the real and imaginary parts, we obtain

$$\begin{aligned}\eta^2 ab - y^2 &= \eta^2 ab \cos(2y) \\ \eta(a+b)y &= -\eta^2 ab \sin(2y)\end{aligned}$$

Squaring and adding these equations leads to

$$y^2 (y^2 + \eta^2 (a^2 + b^2)) = 0.$$

which has no real roots. Thus, there are no roots of the form iy . ■

The distribution of roots in (32) is summarized in Figure 3.

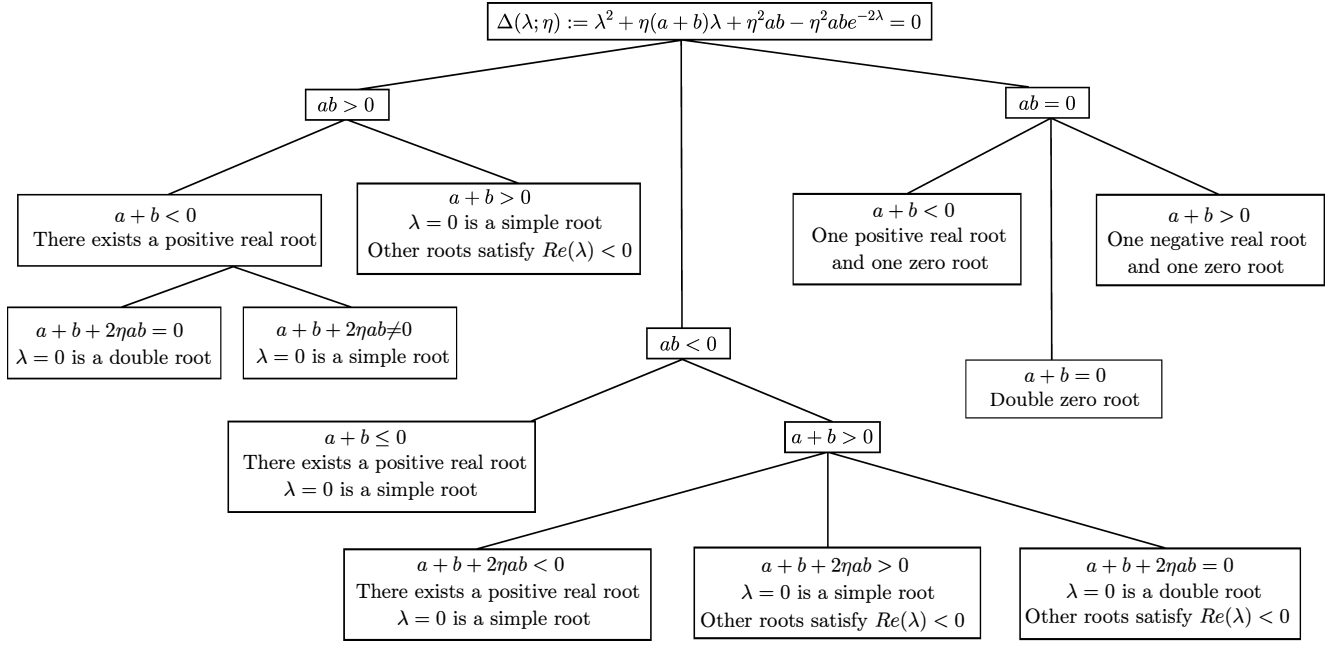


Figure 3: The distribution of roots in (32) as discussed in Propositions 3.1–3.6.

Recall the structure of the phase-locked solutions (21) of the phase model (20). From this we see that a phase-locked periodic solution of the original model (17) corresponds to a line in the phase model (20), that is, when ψ^* and ω^* are solutions of (22), it follows that

$$\begin{cases} \varphi_1 = \omega^* t & (\text{mod } 2\pi) \\ \varphi_2 = \omega^* t + \psi^* & (\text{mod } 2\pi) \end{cases} \Rightarrow \varphi_2 = \varphi_1 + \psi^* \pmod{2\pi}.$$

From Proposition 3.4, we know that for any $\tau > 0$, $\Delta(\lambda; \eta(\tau)) = 0$ has a zero root. The simple zero root corresponds to the motion along these lines. It corresponds to the Floquet multiplier 1 which is associated with the periodic solution of the original model (17). Thus phase-locked solutions will be asymptotically stable if $\lambda = 0$ is a simple root of the characteristic equation (32) and all other roots have negative real part.

Remark 3.1. *The solution $\psi^* \neq 0, \pi$ is asymptotically stable for values of a, b such that $a > 0$ and $b > 0$ or $ab < 0$, $a+b > 0$ and $a+b+2\eta ab > 0$. Since H' is a 2π -periodic function, the solutions ψ^* and $2\pi - \psi^*$ have the same stability.*

Remark 3.2. Since H is a 2π -periodic function, $a = b = \frac{1}{\Omega}H'(\psi^* - \omega^*\eta - \Omega\tau)$ in (30) when $\psi^* = 0, \pi$. Hence, the stability of solutions when $\psi^* = 0, \pi$ is determined by the sign of $H'(\psi^* - \omega^*\eta - \Omega\tau)$, that is, the solution is asymptotically stable when $H'(\psi^* - \omega^*\eta - \Omega\tau) > 0$ and unstable when $H'(\psi^* - \omega^*\eta - \Omega\tau) < 0$.

3.1 Bifurcation

Suppose that Ω and ϵ are fixed, but τ may be varied. From the discussion above, potential bifurcation points of the model (20) are values $\tau = \tau^*$ where the characteristic equation for a particular phase-locked solution, ψ^*, ω^* has a double zero root. Let $\eta^* = \epsilon\Omega\tau^*$. When $\psi^* = 0$ or π there are two types of potential bifurcation points:

- (1) τ^* where $H'(\psi^* - \omega^*\eta^* - \Omega\tau^*) = 0$ (see Remark 3.2);
- (2) τ^* where $1 + \eta^*\frac{1}{\Omega}H'(\psi^* - \omega^*\eta^* - \Omega\tau^*) = 0$ (see Proposition 3.4).

For other values of ψ^* , Proposition 3.4 indicates there is a potential bifurcation point at

- (3) τ^* where $\eta^* = -\frac{a+b}{2ab}$.

Note that it is impossible to find an explicit expression for the bifurcation values because each of these conditions are implicit equations for τ^* .

Now we consider what type of bifurcations may occur at these points. We do not make a rigorous proof, which would require centre manifold and normal form theory. However, we can make some plausible arguments based on the equations for the equilibrium solutions. Recall that (ψ^*, ω^*) with $\psi^* = 0$ or π defines a phase-locked solution at τ if $F(\omega^*, \psi^*; \tau) = 0$ where

$$F(\omega, \psi^*; \tau) = \omega - \frac{1}{\Omega}H(\psi^* - \omega\eta - \Omega\tau).$$

Differentiating F with respect to ω shows that the condition (2) corresponds to $F_\omega(\omega^*, \psi^*; \tau^*) = 0$, that is, ω^* is a double root of F when $\tau = \tau^*$. Thus as τ varies near τ^* we may expect that there should be two roots of F near ω^* or none¹. Thus the bifurcation associated with condition (2) should be a saddle-node bifurcation involving two different phase-locked solutions with the same ψ^* . Note that this bifurcation is only physically relevant if $\eta^* > 0$, i.e., $H'(\psi^* - \omega^*\eta^* - \Omega\tau^*) < 0$. Thus, from Remark 3.2, the associated solutions will be unstable. In a similar manner one can show that condition (3) corresponds to (ψ^*, ω^*) at $\tau = \tau^*$ being a point of tangency of the curves defined by equations (22). Thus we expect it to correspond to a saddle-node bifurcation involving two out-of-phase solutions with different ψ^* . The stability of these solutions will depend on which case of Proposition 3.4 applies. Finally, we consider phase-locked solutions near $\psi = 0$. Expanding equations (25) and the first of (22) in ψ and keeping the two lowest order terms we have

$$0 = 2H'(-\omega\eta - \Omega\tau)\psi + \frac{2}{3}H'''(-\omega\eta - \Omega\tau)\psi^3 \quad (36)$$

$$\omega = \frac{1}{\Omega}(H(-\omega\eta - \Omega\tau) + H'(-\omega\eta - \Omega\tau)\psi). \quad (37)$$

Thus we see that $\psi^* = 0$, $\omega^* = H(-\omega^*\eta - \Omega\tau)/\Omega$, is always a solution of this system and if there is τ^* such that condition (1) is satisfied and $H'''(-\omega^*\eta^* - \Omega\tau^*) \neq 0$ then this will be a triple root of

¹More precisely, we expect this will occur if F satisfies the further conditions $F_\tau(\omega^*, \psi^*; \tau^*) = -\Omega(1 + \epsilon\omega^*)/\eta^* \neq 0$ and $F_{\omega\omega}(\omega^*, \psi^*; \tau^*) = -(\eta^*)^2 H''(\psi^* - \omega^*\eta^* - \Omega\tau^*) \neq 0$ [39].

the system. Thus we expect that condition (1) with $\psi^* = 0$ corresponds to a pitchfork bifurcation where two out-of-phase solutions are created near 0. Similarly condition (1) with $\psi^* = \pi$ should correspond to a pitchfork bifurcation where two out-of-phase solutions are created near π .

Note that the phase interaction function H can be represented by Fourier series expansion

$$H(\phi) = a_0 + \sum_{k=1}^{\infty} [a_k \cos(k\phi) + b_k \sin(k\phi)].$$

When the interaction function H is represented by the first set of Fourier modes

$$H(\phi) = a_0 + a_1 \cos(\phi) + b_1 \sin(\phi), \quad (38)$$

the authors in [36] show that the out-of-phase solutions and pitchfork bifurcation cannot occur in the phase model (20) with small time delay. However, it may occur when the time delay is large. Indeed, when H has the form in (38), then it follows from (22) and (25) that

$$\Omega\omega^* = a_0 + A(\omega^*) \sin(\psi^*) + B(\omega^*) \cos(\psi^*), \quad (39)$$

$$0 = 2A(\omega^*) \sin(\psi^*) \quad (40)$$

respectively, where

$$A(\omega^*) = b_1 \cos(\omega^* \eta + \Omega\tau) + a_1 \sin(\omega^* \eta + \Omega\tau),$$

$$B(\omega^*) = a_1 \cos(\omega^* \eta + \Omega\tau) - b_1 \sin(\omega^* \eta + \Omega\tau).$$

Thus, from $\sin(\psi^*) = 0$, we have that $\psi^* = 0, \pi$ with the corresponding ω^* determined by

$$\Omega\omega^* - a_0 = \pm B(\omega^*). \quad (41)$$

where the + corresponds to $\psi^* = 0$ and the - to $\psi^* = \pi$. Also, from $A(\omega^*) = 0$ we determine ω^* and the corresponding ψ^* is obtained from

$$\cos(\psi^*) = \frac{\Omega\omega^* - a_0}{B(\omega^*)}. \quad (42)$$

Consequently, we have the following cases

- if $|\Omega\omega^* - a_0| < |B(\omega^*)|$, then two out-of-phase solutions ψ^* and $2\pi - \psi^*$ exist,
- if $|\Omega\omega^* - a_0| = |B(\omega^*)|$, then one solution exists ($\psi^* = 0$ or $\psi^* = \pi$),
- if $|\Omega\omega^* - a_0| > |B(\omega^*)|$, then no solution satisfying (42) exists.

Note that $H'(-\omega^* \eta - \Omega\tau) = A(\omega^*)$ and $H'(\pi - \omega^* \eta - \Omega\tau) = -A(\omega^*)$. Thus, the solutions 0 and π change stability when $A(\omega^*) = 0$ where ω^* satisfies (41). As τ varies, out-of-phase solutions will disappear if $\frac{\Omega\omega^* - a_0}{B(\omega^*)} - 1$ changes its sign from negative to positive. When $\frac{\Omega\omega^* - a_0}{B(\omega^*)} = 1$, then $\psi^* = 0$. Hence, a pitchfork bifurcation occurs at $\psi^* = 0$. Similarly when $\frac{\Omega\omega^* - a_0}{B(\omega^*)} = -1$ a pitchfork bifurcation occurs at $\psi^* = \pi$.

3.2 The full model with small delay

When the time delay, τ , in (17) is relatively small, in the sense that $\Omega\tau = \mathcal{O}(1)$, it follows from the theory of averaging that the time delay τ enters the interaction function H in (20) as a phase shift [14, 24, 27, 36]. In [36], the authors considered this case and consequently the time delay η in the phase model (20) was neglected, and hence, it becomes

$$\begin{aligned}\frac{d\varphi_1}{dt} &= \frac{1}{\Omega}H(\varphi_2(t) - \varphi_1(t) - \Omega\tau), \\ \frac{d\varphi_2}{dt} &= \frac{1}{\Omega}H(\varphi_1(t) - \varphi_2(t) - \Omega\tau),\end{aligned}\tag{43}$$

Therefore, they were able to reduce (20) into a one dimensional ordinary differential equation

$$\frac{d\phi}{dt} = -2\epsilon[H(\phi - \Omega\tau) - H(-\phi - \Omega\tau)].\tag{44}$$

where $\phi = \varphi_2 - \varphi_1$. The existence of phase-locked solutions of (44) was discussed in [36] without introducing the frequency deviation ω . Hence, the in-phase and anti-phase solutions were unique. Moreover, the stability of the phase-locked solution ϕ^* in (44) was determined by the sign of

$$\widehat{H}'(\phi^*) := \bar{a} + \bar{b}\tag{45}$$

where $\bar{a} = H'(\phi^* - \Omega\tau)$ and $\bar{b} = H'(-\phi^* - \Omega\tau)$. If $\widehat{H}'(\phi^*) > 0$ then ϕ^* is asymptotically stable and if $\widehat{H}'(\phi^*) < 0$ it is unstable. When $\widehat{H}'(\phi^*) = 0$ the stability is not determined by the linearization.

Remark 3.3. In [36], due to the reduction of the two dimensional system (43) into a single equation (44), the zero root was omitted in characteristic equation. Indeed, the characteristic equation of (44) is $\lambda + \widehat{H}'(\phi^*) = 0$ while the characteristic equation of (43) is

$$\lambda(\lambda + \widehat{H}'(\phi^*)) = 0.\tag{46}$$

It is clear that the latter characteristic equation always has a zero root.

Now we compare these results with what happens when τ is small, i.e., $\Omega\tau = \mathcal{O}(1)$, in our model (20). Recall that $\eta = \epsilon\Omega\tau$ thus the assumption on τ implies that $\eta = \mathcal{O}(\epsilon)$. Also, note that the phase difference ϕ^* of the phase locked solutions for the model (45) is the same as the phase deviation difference ψ^* for our model.

First consider the existence of phase-locked solutions. For our model we must solve the equations (25) and one of (22) simultaneously for ψ and ω . When $\eta = \mathcal{O}(\epsilon)$, however, to first order in ϵ the H function no longer depends on ω . Thus phase-locked solutions are determined by ψ^* satisfying $H_\tau(\psi^*) = 0$, with $\omega^* = \frac{1}{\Omega}H(\psi^* - \Omega\tau)$. This equation for ψ^* is the same as in [36]. In [36] they did not solve for ω^* as it was not needed to determine the phase-locked solutions or their stability. It remains to consider the uniqueness of the in-phase and anti-phase solutions. From equations (26) and (27), these solutions correspond to frequency deviations ω^* satisfying $F(\omega^*, \psi^*) = 0$ with $\psi^* = 0, \pi$, respectively. Since H and H' are continuous and 2π periodic they are bounded. Thus we see that $\lim_{\omega \rightarrow \pm\infty} F(\omega) = \pm\infty$. Further, recalling (28), since $\eta = \mathcal{O}(\epsilon)$, $F_\omega(\omega^*, \psi^*) > 0$. Thus for any τ sufficiently small, there will be a unique frequency deviation ω^* for $\psi^* = 0$ and for $\psi^* = \pi$. This is consistent with the results in [36] which have only one in-phase and anti-phase solution for each value of τ .

Now consider the stability of the phase-locked solutions. Recall that the stability for our model is summarized in Figure 3. When $\eta = \mathcal{O}(\epsilon)$, $\text{sgn}(a + b + ab\eta) \approx \text{sgn}(a + b)$, thus the conditions for stability/instability of phase-locked solutions of our model reduce to the stability if $a + b > 0$ and instability if $a + b < 0$. Further $a \approx \bar{a}$ and $b \approx \bar{b}$, thus the stability results of our model reduce to those of [36] when $\Omega\tau = \mathcal{O}(1)$. The key point is that, regardless of the size of τ , the countable infinity of complex roots of the characteristic equation (32) all have negative real part. Thus the stability of the phase-locked solutions is determined by finitely many real roots, and it is possible for an ordinary differential equation to accurately reflect this stability.

In Section 4.3, we will show numerically that our model with $\Omega\tau = \mathcal{O}(1)$ fully recovers [36, Figure 4b] and [36, Figure 5b].

4 Application to Morris-Lecar oscillators with diffusive coupling

In this section we apply the results from the previous sections to a network of dimensionless Morris-Lecar oscillators with time delayed diffusive coupling, see e.g., [40, 41]. This model is given by

$$\begin{aligned} v_i' &= I_{app} - g_{Ca}m_\infty(v_i)(v_i - v_{Ca}) - g_Kw_i(v_i - v_K) - g_L(v_i - v_L) - \epsilon(v_j(t - \tau) - v_i(t)), \\ w_i' &= \varphi\lambda(v_i)(w_\infty(v_i) - w_i), \end{aligned} \quad (47)$$

for $i, j = 1, 2$ such that $i \neq j$, where

$$\begin{aligned} m_\infty(v) &= \frac{1}{2} (1 + \tanh((v - \nu_1)/\nu_2)), \\ w_\infty(v) &= \frac{1}{2} (1 + \tanh((v - \nu_3)/\nu_4)), \\ \lambda(v) &= \cosh((v - \nu_3)/(2\nu_4)). \end{aligned}$$

Using the parameter set I\II from [36, Table 1], when there is no coupling in the network each oscillator has a unique exponentially asymptotically stable limit cycle with period $T = 23.87 \setminus 13.81$ corresponding to frequency $\Omega = 0.2632 \setminus 0.455$. The normalized system, such that the frequency is 1, corresponding to (47) is

$$\begin{aligned} v_i' &= \frac{1}{\Omega} (I_{app} - g_{Ca}m_\infty(v_i)(v_i - v_{Ca}) - g_Kw_i(v_i - v_K) - g_L(v_i - v_L)) - \frac{\epsilon}{\Omega} (v_j(t - \Omega\tau) - v_i(t)), \\ w_i' &= \frac{1}{\Omega} (\varphi\lambda(v_i)(w_\infty(v_i) - w_i)), \end{aligned} \quad (48)$$

$i = 1, 2$. Note that this is in the form (17) with $\mathbf{X}_i(t) = (v_i(t), w_i(t))^T$ and the function $\mathbf{G} : \mathbb{R}^2 \times \mathbb{R}^2 \rightarrow \mathbb{R}^2$ is given by $\mathbf{G} = (G_1, G_2)$ where $G_1(\mathbf{X}_1(t), \mathbf{X}_2(t)) = \frac{1}{\Omega}(v_2(t - \Omega\tau) - v_1(t))$ and $G_2(\mathbf{X}_1(t), \mathbf{X}_2(t)) = 0$. Then, the phase model interaction function H is given by (19).

For each parameter set, the authors in [36] solved (19) numerically and calculated the approximation of the phase model interaction function H by the first five terms of its Fourier series. These

are given by

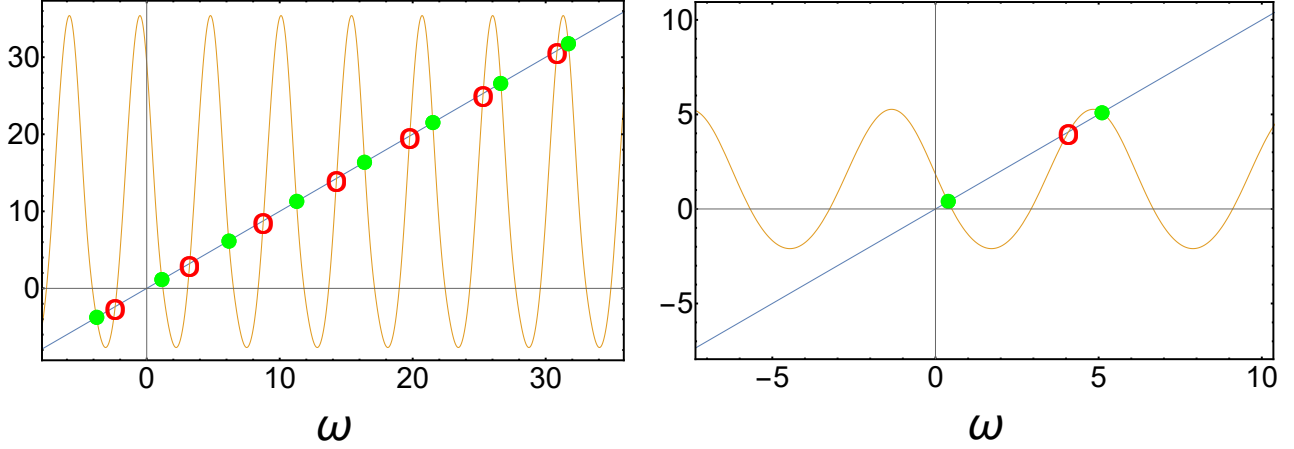
$$\begin{aligned}
H_I(\phi) &= 2.915252 - 2.684797 \cos(\phi) - 0.3278022 \cos(2\phi) \\
&\quad + 0.05596774 \cos(3\phi) + 0.0351635 \cos(4\phi) + 4.908449 \sin(\phi) \\
&\quad - 0.7020183 \sin(2\phi) - 0.09934668 \sin(3\phi) - 0.01104474 \sin(4\phi), \\
H_{II}(\phi) &= 0.6271561 - 0.5209326 \cos(\phi) - 0.08538575 \cos(2\phi) \\
&\quad - 0.005648281 \cos(3\phi) - 0.0002642404 \cos(4\phi) + 1.595618 \sin(\phi) \\
&\quad - 0.04727176 \sin(2\phi) - 0.00301241 \sin(3\phi) - 0.002760313 \sin(4\phi)
\end{aligned} \tag{49}$$

corresponding to the parameter sets I and II, respectively, see [36, Table 2]. Note that the two parameter sets represent limit cycles which are created by different bifurcations as the input current I_{app} is varied. For parameter set I the limit cycle is created in a saddle-node on an invariant circle bifurcation, while for parameter set II the limit cycle is created in a supercritical Hopf bifurcation. The chosen parameter values have I_{app} slightly larger than the bifurcation values.

In [36] the authors studied how small epsilon needed to be for the phase model to faithfully represented the behaviour of the full system (48), in the case of small delay. They found that for parameter set I ϵ could be as large as 0.05 while for parameter set II epsilon should not exceed 0.001. Therefore, in the rest of this section, we take $\epsilon = 0.05$ with parameter set I and $\epsilon = 0.001$ when we use parameter set II. Consequently, we choose $\tau \geq 75.988$ for parameter set I and $\tau \geq 2197.8$ for parameter set II so that $\epsilon\Omega\tau = \mathcal{O}(1)$. Moreover, we compare our results with the results in [36] when the time delay, τ , in (17) is relatively small.

4.1 In-phase and anti-phase solutions

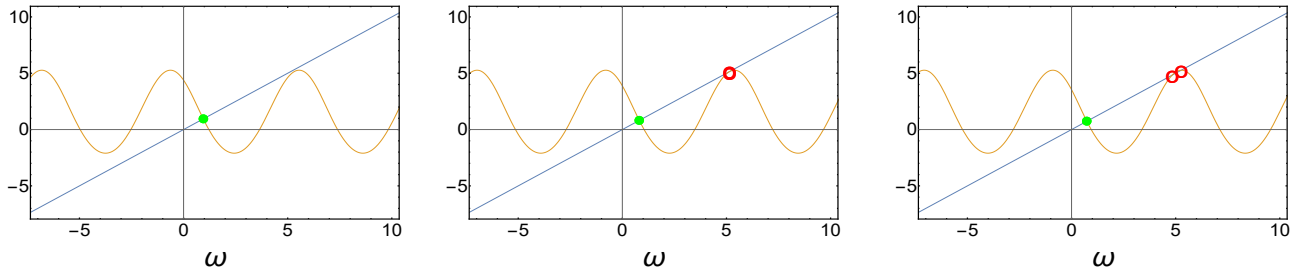
To find ω^* corresponding to the in-phase and anti-phase solutions, $\psi^* = 0, \pi$, we solve (26) and (27) with H given by either H_I or H_{II} from (49). Note that these equations can only be solved numerically due to the complicated form of H_I and H_{II} . For particular values of τ , we represent these solutions graphically in Figure 4 as the intersection points of the line $y = \omega$ and the curve $y = H(-\omega\eta - \Omega\tau)/\Omega$. In (26), the slope of the right hand side at any ω is $\ell_\tau = -\epsilon\tau H'(-\omega\eta - \Omega\tau)$. Then, by applying the stability condition in Remark 3.2, we see that the in-phase solution is stable when the line $y = \omega$ intersects the curve of the function $H(-\omega\eta - \Omega\tau)/\Omega$ at a point where it has negative slope, while it is unstable when the intersection is at a point with positive slope, see Figure 4. When the line $y = \omega$ alternates from intersecting the curve of $H(-\omega\eta - \Omega\tau)/\Omega$ at a point with positive slope to intersecting it at a point with negative slope, the solutions ω^* alternate between stable and unstable, see Figure 4. For fixed Ω and ϵ , as τ increases the curve $H(-\eta\omega - \Omega\tau) = H(-\Omega\tau(1 + \epsilon\omega))$ compresses horizontally causing the creation and destruction of intersection points. For specific values $\tau = \tau_1^* > 0$, an intersection point will occur at the point where the function H has slope one, i.e., the curve $y = H$ will be tangent to the line $y = \omega$ at these values of τ , see Figure 5b. Near such points, i.e., for τ slightly bigger or smaller, there exist two consecutive intersection points both of which are unstable, see Figure 5c. Then, as τ changes further to τ_2^* , one unstable point quickly passes through the point where H has zero slope and becomes stable, see Figure 4b. The values τ_1^* correspond to the saddle-node bifurcations of in-phase and anti-phase solutions discussed in Section 3.1. We will discuss the points τ_2^* later. In Figure 7, we plot ω^* corresponding to $\psi^* = 0, \pi$ for various values of the time delay τ , showing the many co-existing solutions which can occur and the transitions of the solutions as τ varies. These solutions were found by implementing the algorithm from [42] in *Wolfram Mathematica* to find all the solutions of (26) or (27).



(a) $H_I(-\omega\eta - \Omega\tau)/\Omega$ and $y = \omega$. $\tau = 90$.

(b) $H_{II}(-\omega\eta - \Omega\tau)/\Omega$ and $y = \omega$. $\tau = 2236$.

Figure 4: Graphical representation of the solutions to (26) with fixed τ . The circles \bullet/\circ represent stable/unstable solutions.



(a) $\tau = 2234.4$.

(b) $\tau = 2234.78$.

(c) $\tau = 2235$.

Figure 5: Graphical solutions of $H_{II}(-\omega\eta - \Omega\tau)/\Omega$ and $y = \omega$ with fixed τ . The circles \bullet/\circ represent stable/unstable solutions.

To compare prediction of the phase model (20) and solutions of the full model (47), we solve (48) numerically with parameter sets I and II with various values of τ and different initial conditions. The initial conditions are of the form

$$(v_1(t), w_1(t), v_2(t), w_2(t))^T = (v_{10}, w_{10}, v_{20}, w_{20})^T \quad t \in [-\tau\Omega, 0]. \quad (50)$$

Figure 6 shows time series of v_i in (48) with different initial conditions. We notice the coexistence of in-phase solutions with different frequencies when $\tau = 110$ with parameter set I. The numerical solutions are obtained by using *Wolfram Mathematica*. We use the command `NDSolve` to solve the full model numerically.

When $\epsilon = 0$, each uncoupled equation in (48) has 2π -periodic solution, that is, the frequency of each oscillator is unity. Consequently, when $\epsilon \neq 0$ and equation (48) has a phase-locked solution, the phase of the first oscillator is $\theta_1(t) = t + \omega^*\epsilon t$ and that of the second oscillator is $\theta_2(t) = t + \omega^*\epsilon t + \psi^*$ where ω^* is the frequency deviation and ψ^* is the phase shift. Thus, the frequency of each oscillator is $1 + \omega^*\epsilon$, and the period \mathcal{T} is approximately

$$\mathcal{T} = \frac{2\pi}{1 + \omega^*\epsilon}.$$

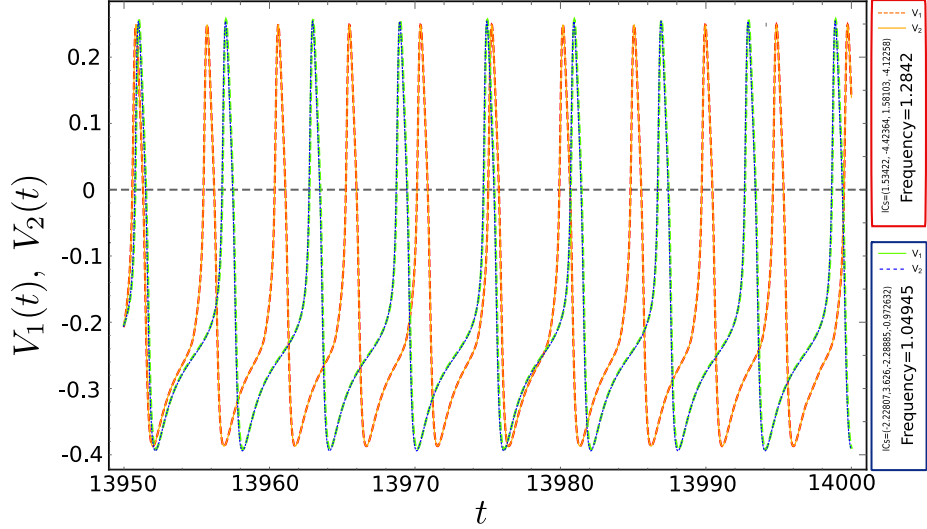


Figure 6: The coexistence of in-phase solutions of (48) with different frequencies when $\tau = 110$ with parameter sets I. We take different initial conditions: $(1.53422, -4.42364, 1.58103, -4.12258)^T$ for red/orange curves and $(-2.22807, 3.626, -2.28885, -0.972632)^T$ for blue/green curves.

From the numerical solution of (48) for a stable phase-locked solution, we can calculate the period \mathcal{T} of the oscillators and determine the approximate frequency deviation from

$$\omega^* \approx \frac{1}{\epsilon} \left(\frac{2\pi}{\mathcal{T}} - 1 \right). \quad (51)$$

Figure 7 shows the coexistence of stable in-phase and anti-phase periodic solutions and demonstrates that the approximation of ω^* from (51) is close to a stable solution of the phase model. The values of ω^* with the normalized error

$$E_N = \frac{(\omega^* \text{ in the phase model}) - (\omega^* \text{ in the full model})}{\omega^* \text{ in the full model}} \quad (52)$$

are shown in Tables 1 and 2. Note that the quantity E_N is the normalized error with respect to the size of ω^* in the full model. Except for a few cases, the phase model gives a very accurate prediction of the values of ω^* . The phase model predicted stable phase-locked solutions that we did not find numerically, however, it is possible that further exploration with different initial conditions might find them.

4.2 Out-of-phase solutions

To find phase-locked solutions other than the in-phase and anti-phase solutions, we fix τ and solve

$$\begin{aligned} \omega^* &= \frac{1}{\Omega} H_{II}(\psi^* - \omega^* \eta - \Omega \tau), \\ \omega^* &= \frac{1}{\Omega} H_{II}(-\psi^* - \omega^* \eta - \Omega \tau) \end{aligned} \quad (53)$$

for ω^* and ψ^* . Figure 8 shows all solutions to (53) when $\tau = 100 \setminus 2205$ with the parameter set I \setminus II. As seen for the existence of in-phase and anti-phase solutions in Section 4.1, the number of phase-locked solutions with the parameter set I is bigger than II. For the purpose of clarity in the bifurcation figures, we consider the parameter set II in this section.

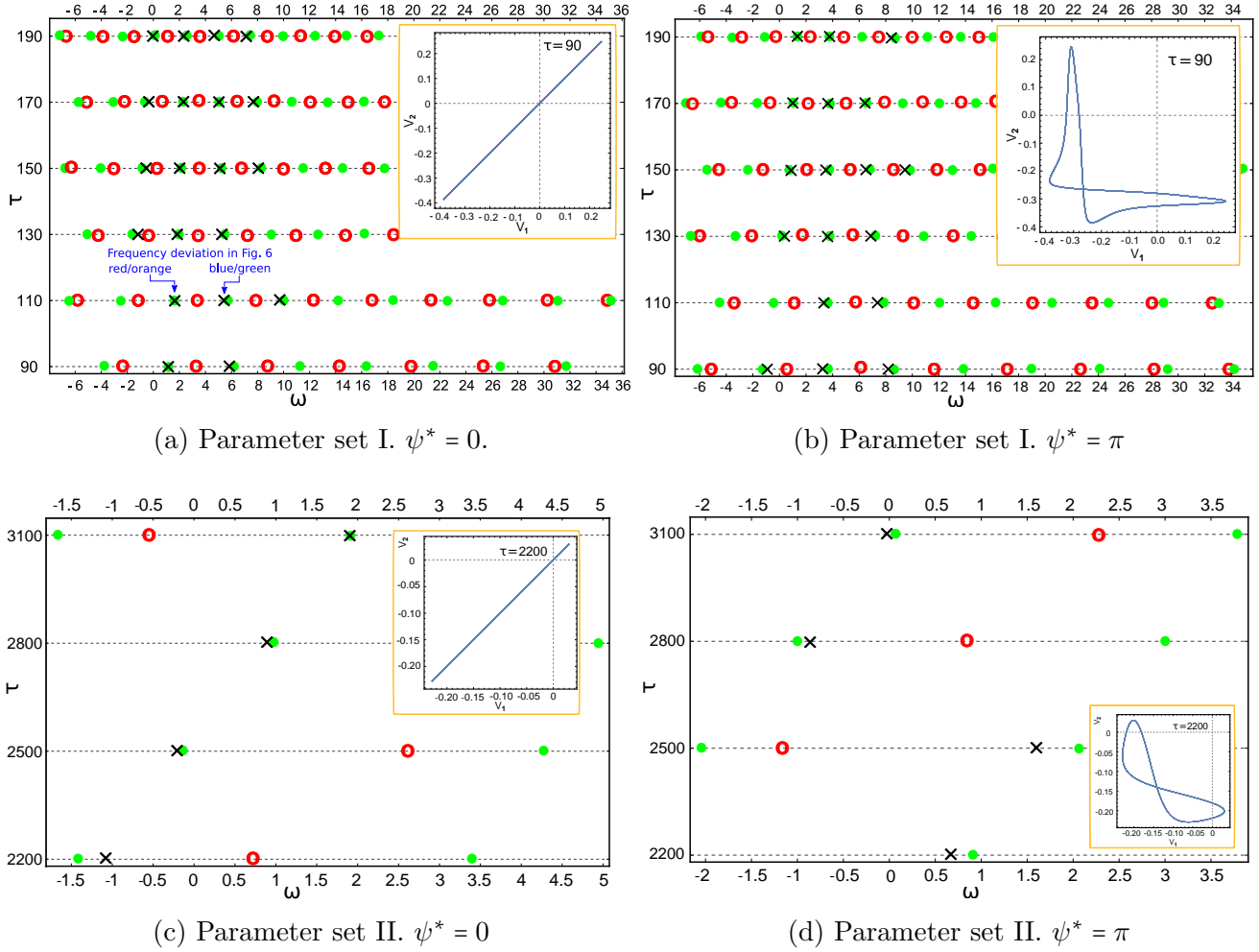


Figure 7: The circles \bullet/\circ represent stable/unstable solutions to the phase model (20) corresponding to (48) and \times represents the calculated ω^* for each stable phase-locked periodic solution found by numerical integration of the full model (48) with parameter sets I and II. The insets are in-phase and anti-phase periodic solutions of (48). The initial conditions for all simulations was of the form (50). For the insets the values of $(v_{10}, w_{10}, v_{20}, w_{20})^T$ are as follows. (a) $(1.53422, -4.42364, 1.58103, -4.12258)^T$ (b) $(1.57882, 4.1827, 2.78262, 0.358165)^T$ (c) $(1.892, -0.296437, -1.05518, 1.09985)^T$ (d) $(-1.72448, -1.46442, 4.4848, 1.31822)^T$

In Figure 8b, we observe that there are four non-trivial phase-locked solutions: $\psi_1^* = 1.85996$ and $\psi_2^* = 2.13981$ in $(0, \pi)$; and $\psi_3^* = 2\pi - \psi_1^* = 4.42323$ and $\psi_4^* = 2\pi - \psi_2^* = 4.14338$ in $(\pi, 2\pi)$. Moreover, we have $\omega_1^* = \omega_3^* = 0.14125$ and $\omega_2^* = \omega_4^* = 0.14125$ where ω_i^* is the corresponding frequency deviation to ψ_i^* , $i = 1, 2, 3, 4$. This agrees with Proposition 2.1.

In Figure 9a, we plot all solutions of system (53) in $\tau\psi$ -plane and mark the stability using the criteria in Section 3. Note that since this representation suppresses ω^* , the multiple in-phase or anti-phase solutions which occur for particular values of τ in Figure 7 are superimposed. As τ varies, we observe that a stable solution corresponding to $\psi^* = 0, \pi$ always exists with the appearance of an unstable solution in disjoint intervals of τ , while all the out-of-phase solutions are unstable. More precisely, for the in-phase solution, as τ increases, we notice that an unstable solution disappears at $\tau \approx 2203$, exists between $\tau \approx 2207.5$ and $\tau \approx 2217$, and reappears at $\tau \approx 2221$. The same behaviour occurs for the anti-phase solution at different values of τ . Near the appearance and disappearance

$\psi^* = 0$									
	$\tau = 90$			$\tau = 110$			$\tau = 130$		
	Phase Model	Full Model	E_N	Phase Model	Full Model	E_N	Phase Model	Full Model	E_N
ω^*	1.1446	0.988971	0.1574	1.61521	1.44374	0.1188	-1.55286	-1.31666	-0.1794
	6.17015	5.68396	0.0855	9.95867	9.67259	0.0296	5.48587	5.16611	0.0619
	$\tau = 150$			$\tau = 170$			$\tau = 190$		
	Phase Model	Full Model	E_N	Phase Model	Full Model	E_N	Phase Model	Full Model	E_N
ω^*	-0.860951	-0.766851	-0.1227	2.38636	2.23525	0.0676	0.101849	0.092197	0.1047
	2.19521	2.03459	0.0789	5.11589	4.87837	0.0487	7.44601	7.16109	0.0398
$\psi^* = \pi$									
	$\tau = 90$			$\tau = 110$			$\tau = 130$		
	Phase Model	Full Model	E_N	Phase Model	Full Model	E_N	Phase Model	Full Model	E_N
ω^*	-1.32864	-1.08976	-0.2192	3.68511	3.39257	0.0862	0.193408	0.169843	0.1387
	8.70987	8.244	0.0565	7.86	7.36178	0.0677	7.26467	6.86785	0.0578
	$\tau = 150$			$\tau = 170$			$\tau = 190$		
	Phase Model	Full Model	E_N	Phase Model	Full Model	E_N	Phase Model	Full Model	E_N
ω^*	0.663926	0.600602	0.1054	1.02812	0.946137	0.0867	3.76194	3.58466	0.0495
	9.92786	9.41424	0.0546	3.74932	3.55154	0.0557	8.67729	8.34016	0.0404

Table 1: Comparison of ω^* between the phase model prediction and the full model (48) when $\psi^* = 0, \pi$ with parameter set I. The quantity E_N is defined in (52).

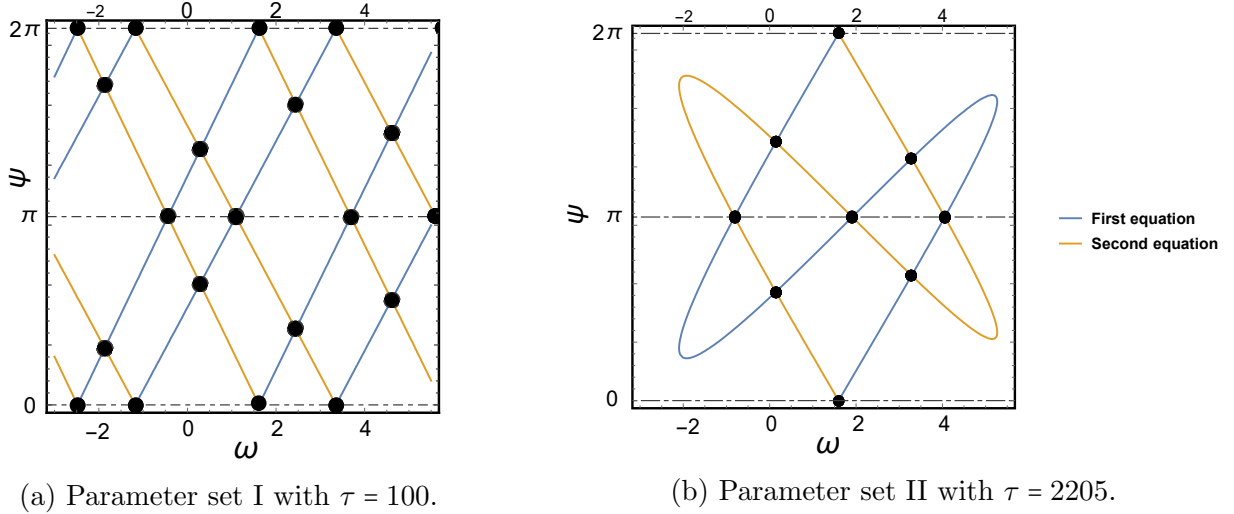


Figure 8: Contour plot of the equations in (53) to show the graphical solutions of (53) with fixed τ .

of these unstable solutions the unstable out-of-phase solutions appear and disappear. As we observe in Figure 8, there are multiple solutions (ω^*, ψ^*) of (53) when τ is fixed. To study the creation and destruction of solutions further, we take particular values for τ and show all solutions in the blue rectangles from Figure 9a in the $\omega\psi$ -plane, see Figures 9b–9i. We now see that there are pitchfork bifurcations where a stable in-phase or anti-phase solution becomes unstable as two unstable out-of-phase solutions merge together, see Figures 9b–9c and 9f–9g. This correspond to the values τ_2^* discussed above. Moreover, there are saddle-node bifurcations where two unstable in-phase or anti-phase solutions collide then vanish, see Figures 9d–9e and 9h–9i. This corresponds to the value τ_1^* discussed above. For other parameter values, we observe the opposite sequence of bifurcations: two unstable in-phase or anti-phase solutions are created by a saddle-node bifurcation after which one gets stabilized by a pitchfork bifurcation involving two unstable out-of-phase solutions. All

$\psi^* = 0$						
	$\tau = 2200$			$\tau = 2500$		
	Phase Model	Full Model	E_N	Phase Model	Full Model	E_N
ω^*	-1.418638	-1.10245	-0.2868	-0.159684	-0.223359	0.2851
	$\tau = 2800$			$\tau = 3100$		
	Phase Model	Full Model	E_N	Phase Model	Full Model	E_N
ω^*	0.9584587	0.720141	0.3309	1.914776	1.880915	0.018
$\psi^* = \pi$						
	$\tau = 2200$			$\tau = 2500$		
	Phase Model	Full Model	E_N	Phase Model	Full Model	E_N
ω^*	0.913646	0.647528	0.411	2.06122	1.58187	0.303
	$\tau = 2800$			$\tau = 3100$		
	Phase Model	Full Model	E_N	Phase Model	Full Model	E_N
ω^*	-1.011297	-0.880915	-0.148	0.0496789	-0.03801	-2.307

Table 2: Comparison of ω^* between the phase model prediction and the full model (48) when $\psi^* = 0, \pi$ with parameter set II. The quantity E_N is defined in (52).

the bifurcations are as predicted for the general model in Section 3.1. We did not observe any saddle-node bifurcations of out-of-phase solutions for this parameter set.

To help understand these bifurcations, we plot solutions in the $\tau\omega$ -plane and the solutions near $\psi = \pi$ in the $\tau\omega\psi$ -space in Figures 10a–10b, respectively. Considering the case $\psi^* = \pi$, we observe that:

- the pitchfork bifurcation occurs when two unstable out-of-phase solutions merge together with one stable anti-phase solution ● to produce one unstable anti-phase solution ■,
- the saddle-node bifurcation occurs when the created unstable anti-phase solution ■ in the above collides with another unstable anti-phase ■ and both vanish.

4.3 Small delay

In this subsection, we consider small time delay, in the sense that, $\Omega\tau = \mathcal{O}(1)$ with respect to the small parameter ϵ , and compare the results with [36] where the authors studied this case using the parameter set II. In [36], the authors studied the dynamics of the phase model corresponding to the full model (17) without introducing the frequency deviation in their analysis because the time delay η was neglected in the phase model when $\Omega\tau = \mathcal{O}(1)$. We have stated some results from [36] in Section 3.2.

As in the previous section we solve (26) and (27) to find ω^* for the in-phase and anti-phase solutions and (53) to find (ψ^*, ω^*) for the out-of-phase solutions. We choose $\tau \in (0, 15)$, which is similar to the range chosen by [36]. In contrast with the results of the last section, here we observe that for $\psi^* = 0, \pi$ there is a *unique* solution ω^* for each τ in the range we considered. This agrees with the prediction of the phase model in Section 3.2. We describe our results in more detail below.

In Figure 11, we plot the in-phase and anti-phase solutions as τ varies in $(0, 15)$ in the $\tau\psi$ -plane. We note that there is similar behaviour in Figure 11a and [36, Figure 4b]. The in-phase and anti-phase solutions change stability as τ increases and their stabilities appear to be the opposite of each other. To examine the behaviour near changes of stability, in Figures 11b–11c we show the

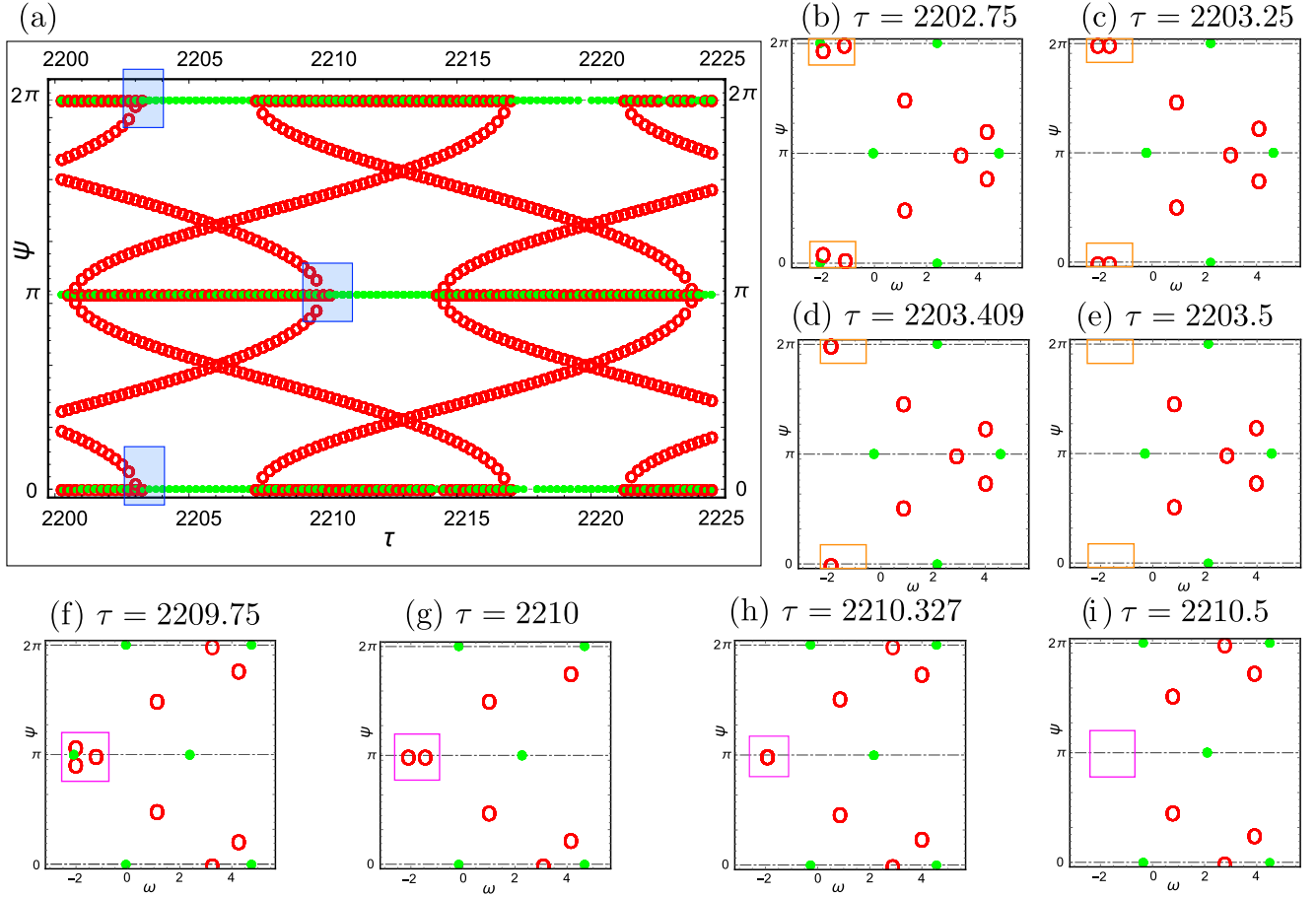


Figure 9: The solutions of phase model (20) corresponding to (48) in the blue rectangles in Figure 10 in $\omega\psi$ -plane. The circles \bullet/\circ represent stable/unstable solutions of (53).

bifurcation diagrams zoomed close to the two switching points. We see that the transition from stable in-phase solution to stable anti-phase solution involves two pitchfork bifurcations and one saddle-node bifurcation of out-of-phase solutions, which agrees with [36]. Figure 13 shows this behaviour when the solutions are plotted in the $\tau\omega$ -plane. Furthermore, we observe in Figures 11b–11c that there are small intervals of τ where bistability occurs. Figure 12 shows the coexistence of stable anti-phase and out-of-phase solutions.

Remark 4.1. *The results in this section are consistent with the results in [27], which indicate that a phase model where the time delay enters as a phase shift is accurate when τ is small in the full model (17) in the sense that $\Omega\tau = \mathcal{O}(1)$ with respect to ϵ for $0 < \epsilon \ll 1$.*

5 Conclusions

In this paper, we studied the phase-locking dynamics of a system of two weakly connected oscillators with time-delayed interaction. By applying the theory of weakly coupled oscillators, we transformed the system into a phase model with an explicit delay in the argument of the phases. We showed that the system always has phase-locked solutions corresponding to in-phase (synchronous, 0 phase difference) and anti-phase (phase difference of half the period) solutions.

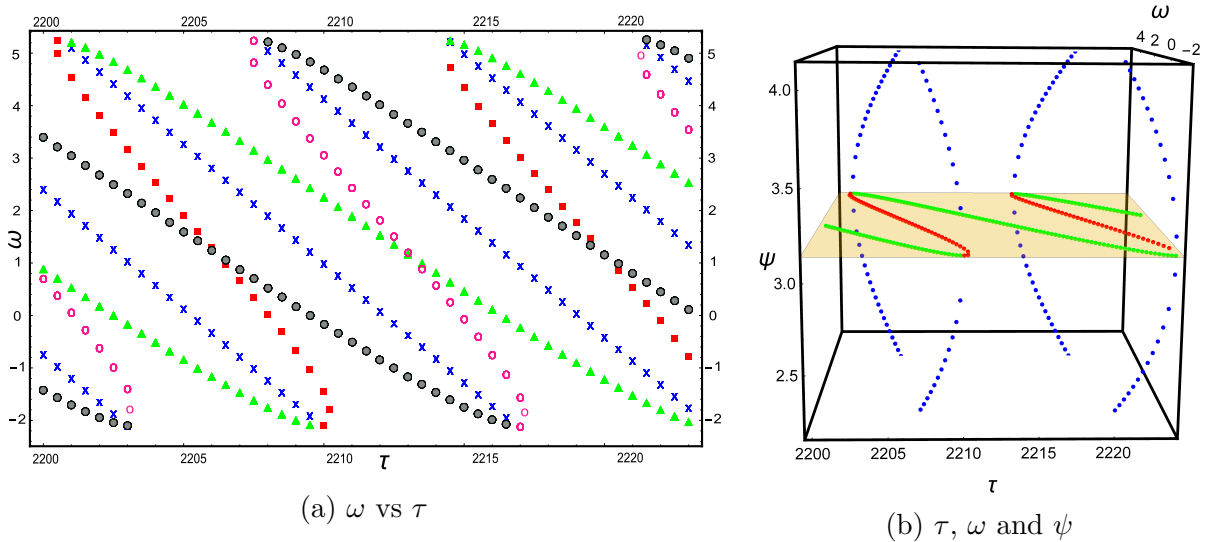


Figure 10: Numerical bifurcation diagram with respect to $\tau \in (2200, 2225)$ for the solutions of the phase model (20) corresponding to the Morris-Lecar model (48) with parameter set II. The circles \bullet/\circ represent stable/unstable in-phase solutions, $\blacktriangle/\blacksquare$ represents stable/unstable anti-phase solutions, and \times represents unstable out-of-phase solutions of (53).

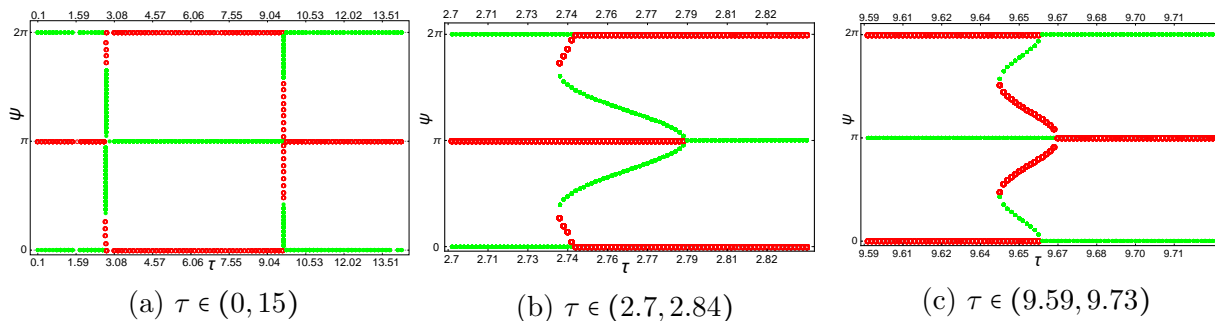


Figure 11: Numerical bifurcation diagram with respect to $\tau \in (0, 15)$ for the phase model (20) corresponding to the Morris-Lecar model (48) with parameter set II. The circles \bullet/\circ represent stable/unstable solutions in the phase model (53).

Further, we showed for small delay ($\Omega\tau = \mathcal{O}(1)$) the in-phase and anti-phase solutions are unique, but for large delay multiple solutions of each type may exist, corresponding to different frequencies. Finally, we showed that phase-locked solutions with any other phase differences (out-of-phase solutions) are also possible. Since the phase model is an infinite-dimensional system of delay differential equations, the linearized system about the phase-locked solutions has a countable infinity of eigenvalues. Through the stability analysis for our model, we discussed the distribution of the eigenvalues on the complex plane to provide stability conditions for the in-phase, anti-phase and out-of-phase solutions. We found that the zero eigenvalue always exists for any choice of parameters and functions which corresponds to the motion along the phase-locked solutions. We showed that the only way in which bifurcations can occur is through the existence of (additional) zero eigenvalues and argued that the following bifurcations may occur: saddle-node bifurcations of two in-phase solutions with different frequencies, saddle-node bifurcations of two anti-phase solutions with different frequencies, saddle-node bifurcations of two different out-of-phase solutions, pitch-fork bifurcations where two out-of-phase solutions arise from an in-phase or anti-phase solution.

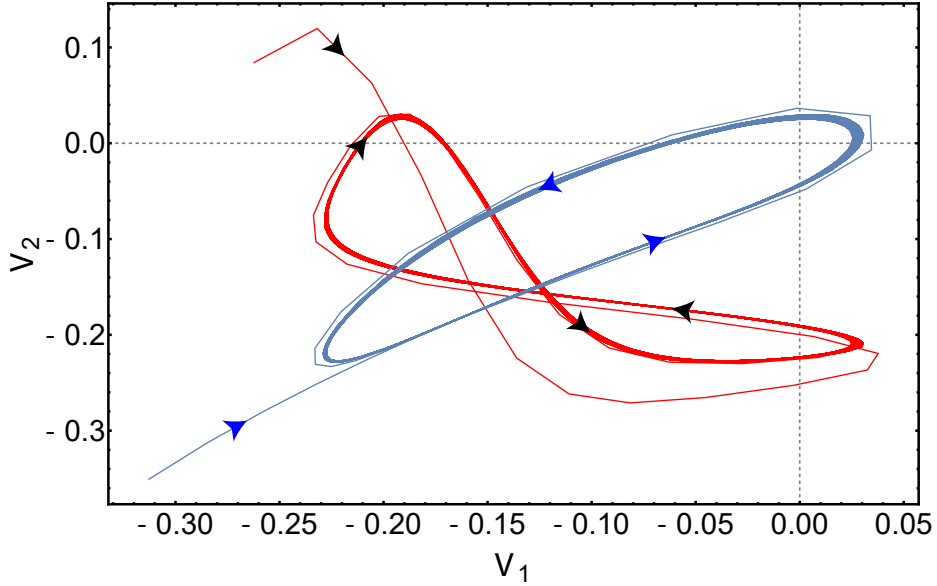


Figure 12: The coexistence of stable anti-phase (red) and out-of-phase (blue) solutions of (48) when $\tau = 9.661$ with parameter sets II. We take different initial conditions: $(0.664192, 0.204054, 5.58914, 0.762568)^T$ for red curve and $(-0.883364, -0.200879, -0.686477, -0.989329)^T$ for blue curve.

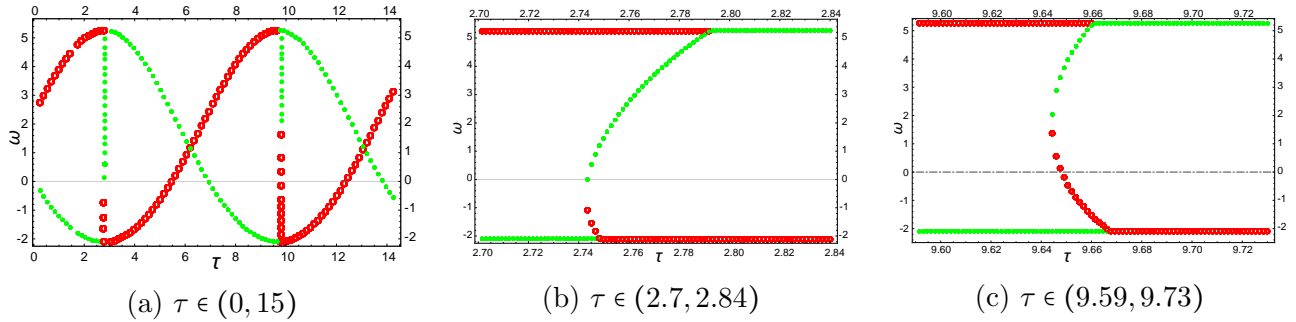


Figure 13: Numerical bifurcation diagram with respect to τ for the phase model (20) corresponding to the Morris-Lecar model (48) with parameter set II. The circles \bullet/\circ represent stable/unstable solutions in the phase model (53).

We showed that the saddle-node bifurcations of in-phase and anti-phase solutions only involve unstable solutions.

Our results on in-phase and anti-phase solutions agree with those in [23, 24], which study the phase model (3), with $n = 2$ and $H(\cdot) = \sin(\cdot)$. We note that they emphasized the need for large coupling-strength for multiple in-phase/anti-phase solutions to exist, however, we show that it is possible with weak coupling and sufficiently large delays. They do not study out-of-phase solutions as these are not possible in their model due to the restriction on H . As can be seen in the literature [8, 9, 11, 12], in order for phase models derived from biophysical oscillator models to adequately capture the dynamics of the full model, the function H generally must include multiple Fourier modes. In [36] it was shown that out-of-phase solutions and pitchfork bifurcations cannot occur in a phase model with small delay if only the first Fourier modes are included in H . However, when the time delay is large, we showed that both out-of-phase solutions and pitchfork bifurcations can occur in the phase model with only the first Fourier modes of H . In general, in the case of large

time delay, the bifurcation structure may change if some modes are dropped. If the coefficients of the modes that are dropped are small, then the bifurcation structure wouldn't change much. The bifurcation points may just move around. If the coefficients of the modes dropped are big enough then there could be large changes in the bifurcation structure.

When the delay is small ($\Omega\tau = \mathcal{O}(1)$), Campbell and Kocbek studied the system

$$\begin{aligned}\frac{d\theta_1}{dt} &= \Omega + \epsilon H(\theta_2(t) - \theta_1(t) - \Omega\tau), \\ \frac{d\theta_2}{dt} &= \Omega + \epsilon H(\theta_1(t) - \theta_2(t) - \Omega\tau),\end{aligned}\tag{54}$$

and proved that in-phase and anti-phase solutions are stable when $H'(\phi^* - \Omega\tau) > 0$, $\phi^* \in \{0, \pi\}$ in [36]. On the other hand, when the time delay is large $\epsilon\Omega\tau = \mathcal{O}(1)$, we proved that these solutions are stable whenever $H'(\phi^* - \omega^*\epsilon\Omega\tau - \Omega\tau) > 0$ where ω^* is the corresponding frequency deviation. It is clear that the stability condition in the first case is independent of the coupling strength parameter and the frequency deviation. Indeed, under the assumption $\theta_1(t) = \Omega + \omega t$ and $\theta_2(t) = \Omega + \omega t + \phi^*$ (see (21)), the terms of the frequency deviation ω will cancel out inside the function H in (54). In fact, in [36], the authors reduce (54) into a single ordinary differential equation and study the dynamics of the model without introducing the frequency deviation. Due to the explicit delay in the phase model, we couldn't reduce the model into a single equation. For the out-of-phase solutions $\phi^* \notin \{0, \pi\}$, the stability condition $H'(\phi^* - \Omega\tau) > 0$ is still valid when the delay is small. While for the large delay the stability becomes more complicated since the explicit delay is an additional parameter that needs to be considered in the phase model.

As an example we considered two Morris-Lecar oscillators with delayed, diffusive coupling. We adopted the parameter values from [36] to compare the results when the time delay is small. We studied the existence and stability of the phase-locked solutions, and explored the bifurcations in the phase model by using a four mode truncation of the Fourier series for the interaction function and compared these results with numerical simulations of the full model. When the time delay τ is large, we found:

- There exist more than one frequency deviation ω corresponding to the in-phase and anti-phase solutions, i.e., co-existence of multiple stable and unstable solutions;
- All out-of-phase solutions are unstable;
- Both the pitchfork and saddle-node bifurcations of in-phase and anti-phase solutions occur.

When the time delay is small, we observed:

- Unique solution in each phase-locked solution category (in-phase, anti-phase and out-of-phase).
- The occurrence of saddle-node bifurcations of out-of-phase solutions and pitchfork bifurcations of in-phase and anti-phase solutions.

Our results agree with [36] when the time delay is small and are consistent with the results in [27], that the explicit time delay can be neglected in the phase model when τ is small.

A special type of phase-locked solutions, so-called *symmetric cluster solutions*, can appear in a network of n identical oscillators, see e.g., [17, 43],

$$\frac{d\mathbf{X}_i}{dt} = \mathbf{F}(\mathbf{X}_i(t)) + \epsilon \sum_{j=1}^n a_{ij} \mathbf{G}(\mathbf{X}_i(t), \mathbf{X}_j(t - \tau)), \quad i = 1, \dots, n, \quad \mathbf{X}_i \in \mathbb{R}^m.\tag{55}$$

In these solutions, also called travelling wave solutions, oscillators in the same cluster are synchronized while those in different clusters have non-zero phase-difference. In [17], Campbell and Wang determined conditions for existence and stability of symmetric cluster solutions in (55) when τ is small and the coupling matrix is circulant. Stability conditions for cluster solutions in networks with small distance dependent delays and random, nearest neighbour coupling have been formulated by several authors (see [24, 37] and references therein). When the time delay is large, Earl and Strogatz provided the stability condition for the in-phase solution ($\theta_i(t) = \Omega t$, i.e., one cluster solution), see [18]. For future research, it would be interesting to study the existence and stability of symmetric cluster solutions in (55) with large time delay.

Acknowledgments

The authors would like to thank the anonymous referees for their careful reading and helpful suggestions.

Appendix: Phase reduction

Assume that the system (10) admits an exponentially asymptotically stable periodic orbit with natural frequency Ω when $\epsilon = 0$. It follows from the time rescaling $\rho \rightarrow \Omega\rho$ that the natural frequency of the periodic orbit becomes 1 and (10) can be written as

$$\frac{d\mathbf{X}_i}{d\rho} = \frac{1}{\Omega}\mathbf{F}(\mathbf{X}_i(\rho)) + \frac{\epsilon}{\Omega}\sum_{j=1}^n K_{ij}\mathbf{G}(\mathbf{X}_i(\rho), \mathbf{X}_j(\rho - \Omega\tau)), \quad i = 1, \dots, n, \quad \mathbf{X}_i \in \mathbb{R}^m \quad (\text{A.1})$$

Consequently, there exists a normally hyperbolic invariant manifold $M = \gamma \times \dots \times \gamma$ of system (A.1) when $\epsilon = 0$, where γ is an exponentially orbitally stable 2π -periodic solution of

$$\frac{d\mathbf{X}_i}{d\rho} = \frac{1}{\Omega}\mathbf{F}(\mathbf{X}_i(\rho)) \quad i = 1, \dots, n. \quad (\text{A.2})$$

Hence, the solution of the i^{th} equation of (A.1) in an ϵ neighborhood of M can be written as

$$\mathbf{X}_i(\rho) = \gamma(\rho + \varphi_i(t)) + \epsilon P_i(\rho, \varphi_1(t), \dots, \varphi_n(t), \epsilon) \quad (\text{A.3})$$

where the term ϵP_i is a smooth vector function which denotes the deviation from the manifold M in the normal plane.

Recall that $t = \epsilon\rho$ and let $\eta := \epsilon\Omega\tau$, then the substitution of (A.3) in (A.1) gives

$$\begin{aligned} \frac{d\mathbf{X}_i}{d\rho} &= \frac{1}{\Omega}\mathbf{F}[\gamma(\rho + \varphi_i(t)) + \epsilon P_i(\rho, \varphi_1(t), \dots, \varphi_n(t), \epsilon)] \\ &+ \frac{\epsilon}{\Omega}\sum_{j=1}^n K_{ij}\mathbf{G}[\gamma(\rho + \varphi_i(t)) + \epsilon P_i(\rho, \varphi_1(t), \dots, \varphi_n(t), \epsilon), \\ &\quad \gamma(\rho - \Omega\tau + \varphi_j(t - \eta)) + \epsilon P_j(\rho, \varphi_1(t - \eta), \dots, \varphi_n(t - \eta), \epsilon)]. \end{aligned} \quad (\text{A.4})$$

Due to the infinite differentiability of \mathbf{F} and \mathbf{G} , it follows from (A.4) that

$$\begin{aligned} \frac{d\mathbf{X}_i}{d\rho} &= \frac{1}{\Omega}\mathbf{F}[\gamma(\rho + \varphi_i(t))] + \frac{\epsilon}{\Omega}D\mathbf{F}[\gamma(\rho + \varphi_i(t))]P_i(\rho, \varphi_1(t), \dots, \varphi_n(t), \epsilon) \\ &+ \frac{\epsilon}{\Omega}\sum_{j=1}^n K_{ij}\mathbf{G}[\gamma(\rho + \varphi_i(t)), \gamma(\rho - \Omega\tau + \varphi_j(t - \eta))] + \mathcal{O}(\epsilon^2) \end{aligned} \quad (\text{A.5})$$

where $D\mathbf{F}$ is the Jacobian matrix of \mathbf{F} .

Now, we differentiate \mathbf{X}_i in (A.3) with respect to ρ to have

$$\frac{d\mathbf{X}_i}{d\rho} = \gamma'(\rho + \varphi_i(t)) \left(1 + \epsilon \frac{d\varphi_i}{dt}\right) + \epsilon \frac{\partial P_i(\rho, \varphi_1(t), \dots, \varphi_n(t), \epsilon)}{\partial \rho} + \mathcal{O}(\epsilon^2). \quad (\text{A.6})$$

Note that

$$\gamma'(\rho + \varphi_i(t)) = \frac{1}{\Omega} \mathbf{F}[\gamma(\rho + \varphi_i(t))]. \quad (\text{A.7})$$

Thus, from (A.5) and (A.6), we obtain

$$\begin{aligned} \mathbf{F}[\gamma(\rho + \varphi_i(t))] \frac{d\varphi_i(t)}{dt} + \Omega \frac{\partial y_i(\rho, \varphi_1(t), \dots, \varphi_n(t))}{\partial \rho} &= D\mathbf{F}[\gamma(\rho + \varphi_i(t))] y(\rho, \varphi_1(t), \dots, \varphi_n(t)) \\ &+ \sum_{j=1}^n K_{ij} \mathbf{G}[\gamma(\rho + \varphi_i(t)), \gamma(\rho - \Omega\tau + \varphi_j(t - \eta))] + \mathcal{O}(\epsilon) \end{aligned} \quad (\text{A.8})$$

where $y_i(\rho, \varphi_1(t), \dots, \varphi_n(t)) := P_i(\rho, \varphi_1(t), \dots, \varphi_n(t), 0) + \mathcal{O}(\epsilon)$ because P_i is smooth function of ϵ . Consequently, since $t = \epsilon\rho$, we replace $\frac{\partial y_i}{\partial \rho}$ by $\frac{dy_i}{d\rho}$ in (A.8). Hence, we can write (A.8) as:

$$\frac{dy_i}{d\rho} = A(\rho, \varphi_i) y + b_i(\rho, \varphi_1, \dots, \varphi_n) + \mathcal{O}(\epsilon) \quad (\text{A.9})$$

where φ_i is $\varphi_i(t)$,

$$A(\rho, \varphi_i) = \frac{1}{\Omega} \mathbf{F}[\gamma(\rho + \varphi_i(t))]$$

and

$$b_i(\rho, \varphi_1, \dots, \varphi_n) = \frac{1}{\Omega} \left[\left(\sum_{j=1}^n K_{ij} \mathbf{G}[\gamma(\rho + \varphi_i(t)), \gamma(\rho - \Omega\tau + \varphi_j(t - \eta))] \right) - \mathbf{F}[\gamma(\rho + \varphi_i(t))] \frac{d\varphi_i(t)}{dt} \right].$$

Since $\varphi_i(t)$ and $\varphi_i(t - \eta)$ in b do not depend directly on ρ , we have a linear non-homogeneous system for y_i , where both the matrix A and the vector b_i are 2π periodic in ρ .

To study existence and uniqueness of solutions to (A.9), we consider the adjoint linear homogeneous system

$$\frac{dQ_i(\rho, \varphi_i)}{d\rho} = -A(\rho, \varphi_i)^T Q_i(\rho, \varphi_i) \quad (\text{A.10})$$

with the normalization condition:

$$\frac{1}{2\pi} \int_0^{2\pi} Q_i^T(\rho, \varphi_i) \mathbf{F}[\gamma(\rho + \varphi_i)] d\rho = 1. \quad (\text{A.11})$$

Since the limit cycle γ is exponentially orbitally stable, the homogeneous ($b_i \equiv 0$) linear system of the form (A.9) the adjoint system (A.10) both have 1 as a simple Floquet multiplier, and all the other multipliers lie inside the unit circle. Thus, system (A.10)-(A.11) has a unique nontrivial periodic solution $q_i(\rho, \varphi_i)$.

Now, by the Fredholm alternative, the linear non-homogeneous system (A.9) has a unique periodic solution Y_i if and only if the following orthogonality condition holds:

$$\langle q_i, b_i \rangle + \mathcal{O}(\epsilon) = \frac{1}{2\pi} \int_0^{2\pi} q_i^T(\rho, \varphi_i) b_i(\rho, \varphi_1, \dots, \varphi_n) d\rho + \mathcal{O}(\epsilon) = 0. \quad (\text{A.12})$$

Assume that $q_i(\rho, 0)$ is found. Hence, $q_i(\rho, \varphi_i) = q_i(\rho + \varphi_i, 0)$ because $A(\rho, \varphi_i) = \frac{1}{\Omega} D\mathbf{F}[\gamma(\rho + \varphi_i(t))] = A(\rho + \varphi_i(t))$. Thus, when we substitute b_i in (A.12), we obtain the following:

$$\begin{aligned} \frac{1}{2\pi\Omega} \int_0^{2\pi} q_i^T(\rho + \varphi_i, 0) \left(\sum_{j=1}^n K_{ij} \mathbf{G}[\gamma(\rho + \varphi_i(t)), \gamma(\rho - \Omega\tau + \varphi_j(t - \eta))] \right) d\rho + \mathcal{O}(\epsilon) \\ = \frac{1}{2\pi} \int_0^{2\pi} q_i^T(\rho + \varphi_i, 0) D\mathbf{F}[\gamma(\rho + \varphi_i(t))] \frac{d\varphi_i(t)}{dt} d\rho. \end{aligned}$$

Since $\frac{d\varphi_i(t)}{dt}$ is treated as a parameter and is independent of ρ , it follows from the normalization condition (A.11) that

$$\frac{d\varphi_i(t)}{dt} = \frac{1}{2\pi\Omega} \int_0^{2\pi} q_i^T(\rho + \varphi_i, 0) \left(\sum_{j=1}^n K_{ij} \mathbf{G}[\gamma(\rho + \varphi_i(t)), \gamma(\rho - \Omega\tau + \varphi_j(t - \eta))] \right) d\rho + \mathcal{O}(\epsilon)$$

Letting $s = \rho + \varphi_i$ leads to

$$\frac{d\varphi_i(t)}{dt} = \frac{1}{2\pi\Omega} \sum_{j=1}^n K_{ij} \left(\int_0^{2\pi} q_i^T(s, 0) \mathbf{G}[\gamma(s), \gamma(s - \Omega\tau + \varphi_j(t - \eta) - \varphi_i(t))] ds \right) + \mathcal{O}(\epsilon)$$

Define

$$H(\varphi_j(t - \eta) - \varphi_i(t) - \Omega\tau) = \frac{1}{2\pi} \int_0^{2\pi} q_i^T(s, 0) \mathbf{G}[\gamma(s), \gamma(s - \Omega\tau + \varphi_j(t - \eta) - \varphi_i(t))] ds.$$

Thus, we have system (11) with

$$\frac{d\varphi_i(t)}{dt} = \frac{1}{\Omega} \sum_{j=1}^n K_{ij} H(\varphi_j(t - \eta) - \varphi_i(t) - \Omega\tau) + \mathcal{O}(\epsilon). \quad (\text{A.13})$$

Recall that $\eta = \epsilon\Omega\tau$. Hence, when $\Omega\tau = \mathcal{O}(1)$ with respect to ϵ , we have

$$\varphi_i(t - \eta) = \varphi_i(t - \epsilon\Omega\tau) = \varphi_i(t) + \mathcal{O}(\epsilon), \quad i = 1, \dots, n.$$

Consequently, the Taylor series expansion for h with respect to ϵ gives

$$\begin{aligned} H(\varphi_j(t - \epsilon\Omega\tau) - \varphi_i(t) - \Omega\tau) &= H(\varphi_j(t) - \varphi_i(t) - \Omega\tau + \mathcal{O}(\epsilon)) \\ &= H(\varphi_j(t) - \varphi_i(t) - \Omega\tau) + \mathcal{O}(\epsilon), \end{aligned}$$

that is, no delay appears in the argument of the phases. Hence, (A.13) becomes:

$$\frac{d\varphi_i(t)}{dt} = \frac{1}{\Omega} \sum_{j=1}^n K_{ij} H(\varphi_j(t) - \varphi_i(t) - \Omega\tau) + \mathcal{O}(\epsilon). \quad (\text{A.14})$$

References

- [1] Y. Kuramoto, *Chemical Oscillations, Waves, and Turbulence*. New York: Springer-Verlag, 1984.
- [2] R. E. Mirollo and S. H. Strogatz, “Synchronization of pulse-coupled biological oscillators,” *SIAM J. Appl. Math.*, vol. 50, no. 6, pp. 1645–1662, 1990.
- [3] H. G. Winful and S. S. Wang, “Stability of phase locking in coupled semiconductor laser arrays,” *Appl. Phys. Lett.*, vol. 53, no. 20, pp. 1894–1896, 1988.
- [4] S. S. Wang and H. G. Winful, “Dynamics of phase-locked semiconductor laser arrays,” *Appl. Phys. Lett.*, vol. 52, no. 21, pp. 1774–1776, 1988.
- [5] F. Dörfler, M. Chertkov, and F. Bullo, “Synchronization in complex oscillator networks and smart grids,” *Proceedings of the National Academy of Sciences*, vol. 110, no. 6, pp. 2005–2010, 2013.
- [6] N. Kopell and G. B. Ermentrout, “Coupled oscillators and the design of central pattern generators,” *Math. Biosci.*, vol. 90, no. 1-2, pp. 87–109, 1988.
- [7] D. Hansel, G. Mato, and C. Meunier, “Phase dynamics for weakly coupled Hodgkin-Huxley neurons,” *Europhys. Lett.*, vol. 23, no. 5, pp. 367–372, 1993.
- [8] S. M. Crook, G. B. Ermentrout, M. C. Vanier, and J. M. Bower, “The role of axonal delay in the synchronization of networks of coupled cortical oscillators,” *Journal of computational neuroscience*, vol. 4, no. 2, pp. 161–172, 1997.
- [9] Y. Park and B. Ermentrout, “Weakly coupled oscillators in a slowly varying world,” *Journal of computational neuroscience*, vol. 40, no. 3, pp. 269–281, 2016.
- [10] A. Takamatsu, T. Fujii, and I. Endo, “Time delay effect in a living coupled oscillator system with plasmodium of *physarum polycephalum*,” *Phys. Rev. E*, vol. 85, no. 9, pp. 2026–2029, 2000.
- [11] E. Wall, F. Guichard, and A. R. Humphries, “Synchronization in ecological systems by weak dispersal coupling with time delay,” *Theoretical ecology*, vol. 6, no. 4, pp. 405–418, 2013.
- [12] Y. X. Zhang, F. Lutscher, and F. Guichard, “How robust is dispersal-induced spatial synchrony?,” *Chaos: An Interdisciplinary Journal of Nonlinear Science*, vol. 25, no. 3, p. 036402, 2015.
- [13] F. Dörfler and F. Bullo, “Synchronization in complex networks of phase oscillators: a survey,” *Automatica*, vol. 50, pp. 1539–1564, 2014.
- [14] F. C. Hoppensteadt and E. M. Izhikevich, *Weakly Connected Neural Networks*, vol. 126. New York: Springer-Verlag, 1997.
- [15] M. Porter and J. P. Gleeson, *Dynamical Systems on Networks: A Tutorial*. Springer, 2016.
- [16] M. A. Schwemmer and T. J. Lewis, “The theory of weakly coupled oscillators,” in *Phase Response Curves in Neuroscience* (N. W. Schultheiss, A. A. Prinz, and R. J. Butera, eds.), pp. 3–31, New York: Springer, 2012.

- [17] S. A. Campbell and Z. Wang, “Phase models and clustering in networks of oscillators with delayed coupling,” *Physica D*, vol. 363, pp. 44–55, 2018.
- [18] M. G. Earl and S. H. Strogatz, “Synchronization in oscillator networks with delayed coupling: A stability criterion,” *Phys. Rev. E*, vol. 67, no. 3, p. 036204, 2003.
- [19] S. Kim, S. H. Park, and C. S. Ryu, “Multistability in coupled oscillator systems with time delay,” *Phys. Rev. Lett.*, vol. 79, no. 15, pp. 2911–2914, 1997.
- [20] T. Luzyanina, “Synchronization in an oscillator neural network model with time-delayed coupling,” *Network: Computation in Neural Systems*, vol. 6, pp. 43–59, 1995.
- [21] E. Niebur, H. Schuster, and D. Kammen, “Collective frequencies and metastability in networks of limit-cycle oscillators with time delay,” *Phys. Rev. Lett.*, vol. 67, pp. 2753–2756, 1991.
- [22] M. K. Yeung and S. H. Strogatz, “Time delay in the Kuramoto model of coupled oscillators,” *Phys. Rev. Lett.*, vol. 82, no. 3, pp. 648–651, 1999.
- [23] H. Schuster and P. Wagner, “Mutual entrainment of two limit cycle oscillators with time delayed coupling,” *Prog. Theor. Phys.*, vol. 82, no. 5, pp. 939–945, 1989.
- [24] B. Ermentrout and T. W. Ko, “Delays and weakly coupled neuronal oscillators,” *Philos. Trans. R. Soc. A-Math. Phys. Eng. Sci.*, vol. 367, no. 1891, pp. 1097–1115, 2009.
- [25] M. Brede and A. C. Kalloniatis, “Frustration tuning and perfect phase synchronization in the Kuramoto-Sakaguchi model,” *Phys. Rev. E*, vol. 93, no. 6, p. 062315, 2016.
- [26] H. Sakaguchi and Y. Kuramoto, “A soluble active rotator model showing phase transitions via mutual entertainment,” *Prog. Theor. Phys.*, vol. 76, no. 3, pp. 576–581, 1986.
- [27] E. M. Izhikevich, “Phase models with explicit time delays,” *Phys. Rev. E*, vol. 58, no. 1, pp. 905–908, 1998.
- [28] B. Ermentrout, “An introduction to neural oscillators,” in *Neural modeling and neural networks* (F. Ventriglia, ed.), pp. 79–110, Oxford, UK: Pergamon Press, 1994.
- [29] G. Ermentrout and D. Terman, *Mathematical Foundations of Neuroscience*. New York, NY: Springer, 2010.
- [30] N. Kopell and G. Ermentrout, “Mechanisms of phase-locking and frequency control in pairs of coupled neural oscillators,” in *Handbook of Dynamical Systems, vol 2: Toward Applications* (B. Fiedler, ed.), pp. 3–54, Amsterdam: Elsevier, 2002.
- [31] R. F. Galán, “The phase oscillator approximation in neuroscience: an analytical framework to study coherent activity in neural networks,” in *Coordinated Activity in the Brain*, pp. 65–89, Springer, 2009.
- [32] T. Zahid and F. Skinner, “Predicting synchronous and asynchronous network groupings of hippocampal interneurons coupled with dendritic gap junctions,” *Brain Research*, vol. 1262, pp. 115–129, 2009.

- [33] B. Pietras and A. Daffertshofer, “Network dynamics of coupled oscillators and phase reduction techniques,” *Phys. Rep.*, 2019.
- [34] H. Nakao, “Phase reduction approach to synchronisation of nonlinear oscillators,” *Contemp. Phys.*, vol. 57, no. 2, pp. 188–214, 2016.
- [35] P. Ashwin, S. Coombes, and R. Nicks, “Mathematical frameworks for oscillatory network dynamics in neuroscience,” *J. Math. Neurosci.*, vol. 6, no. 1, p. 2, 2016.
- [36] S. A. Campbell and I. Kochelevskiy, “Phase models and oscillators with time delayed coupling,” *Discret. Contin. Dyn. Syst. Ser. A*, vol. 8, pp. 2653–2673, 2012.
- [37] T.-W. Ko, S.-O. Jeong, and H.-T. Moon, “Wave formation by time delays in randomly coupled oscillators,” *Phys. Rev. E*, vol. 69, no. 5, p. 056106, 2004.
- [38] A. Pikovsky and M. Rosenblum, “Synchronization,” *Scholarpedia*, vol. 2, no. 12, p. 1459, 2007.
- [39] Y. A. Kuznetsov, *Elements of Applied Bifurcation Theory*. New York: Springer, 1998.
- [40] A. Prasad, S. K. Dana, R. Karnatak, J. Kurths, B. Blasius, and R. Ramaswamy, “Universal occurrence of the phase-flip bifurcation in time-delay coupled systems,” *Chaos*, vol. 18, no. 2, p. 023111, 2008.
- [41] N. Burić and D. Todorović, “Dynamics of Fitzhugh-Nagumo excitable systems with delayed coupling,” *Phys. Rev. E*, vol. 67, no. 6, p. 066222, 2003.
- [42] S. K. Rahimian, F. Jalali, J. Seader, and R. E. White, “A new homotopy for seeking all real roots of a nonlinear equation,” *Computers & chemical engineering*, vol. 35, no. 3, pp. 403–411, 2011.
- [43] K. Okuda, “Variety and generality of clustering in globally coupled oscillators,” *Physica D*, vol. 63, pp. 424–436, 1993.